Anthropogenic Effects on Biogenic Secondary Organic Aerosol Formation

Li XU[1], Lin DU[*1], Narcisse T. TSONA[1], and Maofa GE[2]

[1]*Environment Research Institute, Shandong University, Qingdao 266237, China*

[2]*State Key Laboratory for Structural Chemistry of Unstable and Stable Species, CAS Research/Education Center for Excellence in Molecular Sciences, Institute of Chemistry, Chinese Academy of Sciences, Beijing 100190, China*

ABSTRACT

Anthropogenic emissions alter biogenic secondary organic aerosol (SOA) formation from naturally emitted volatile organic compounds (BVOCs). We review the major laboratory and field findings with regard to effects of anthropogenic pollutants (NOx, anthropogenic aerosols, SO_2, NH_3) on biogenic SOA formation. NOx participate in BVOCs oxidation through changing the radical chemistry and oxidation capacity, leading to a complex SOA composition and yield sensitivity towards NOx level for different or even specific hydrocarbon precursors. Anthropogenic aerosols act as an important intermedium for the gas-particle partition and particle-phase reactions, processes of which are influenced by the particle phase state, acidity, water content and thus associated with biogenic SOA mass accumulation. SO_2 modifies biogenic SOA formation mainly through sulfuric acid formation and accompanies new particle formation and acid-catalyzed heterogeneous reactions. Some new SO_2-involved mechanisms for organosulfates formation have also been proposed. NH_3/amines as the most prevalent base species in the atmosphere, influences biogenic SOA composition

*Corresponding author: Lin DU
Email: lindu@sdu.edu.cn

and modify the optical properties of SOA. The response of SOA formation behavior to these anthropogenic pollutants varies among different BVOCs precursors. Investigations on anthropogenic-biogenic interactions in some areas of China that are simultaneously influenced by anthropogenic and biogenic emissions are summarized. Based on this review, some recommendations are made for a more accurate assessment of controllable biogenic SOA formation and its contribution to the total SOA budget. This study also highlights the importance of controlling anthropogenic pollutant emissions with effective pollutants mitigation policies to reduce regional and global biogenic SOA formation.

Key words: biogenic volatile organic compounds, anthropogenic pollutants, secondary organic aerosol, anthropogenic-biogenic interactions, China

https://doi.org/10.1007/s00376-020-0284-3

Article Highlights:

- Anthropogenic pollutants participate in the gas- and particle-phase reactions to influence biogenic secondary organic aerosol formation, and the detailed mechanism are summarized.
- Anthropogenic effects on biogenic secondary organic aerosol formation exhibit regional and seasonal variations in China, and the observation and modeling evidence are introduced.
- Controlling anthropogenic pollutants benefit the control of biogenic secondary organic aerosol, and suggestions for further research on anthropogenic-biogenic interactions are given.

1. Introduction

Aerosol pollution represents one of the greatest environmental issues of widespread public concern due to its potential impacts on climate change, human health, and air quality (Liao et al., 2014; Lelieveld et al., 2015; von Schneidemesser et al., 2015; Zhang et al., 2015b). Secondary organic aerosols (SOA) that comprise up to 60% of the total aerosol mass have attracted particular attention in recent decades (Riipinen et al., 2012; Huang et al., 2014; Glasius and Goldstein, 2016). Considering that volatile organic compounds (VOCs) are key precursors for SOA formation, efforts have been devoted to incorporate more VOCs sources into atmospheric models. Fossil fuel combustion and evaporation, biomass and biofuel burning and non-combustion related emissions from vegetation and human activities are commonly classified sources (Hoyle et al., 2011; Ensberg et al., 2014; Kelly et al., 2018). Besides these VOC precursors, recent studies have intended to resolve additional SOA sources, including semi-volatile and intermediate-volatility organic compounds (S/IVOCs) (Hayes et al., 2015; Tsimpidi et al., 2016), primary organic aerosol (POA) that is treated as semi-volatility rather than non-volatility (May et al., 2013; Cappa et al., 2016), multi-generational ageing processes (Jathar et al., 2016), and heterogeneous SOA production in organic aerosol (OA) within the cloud- and aerosol-phases (Ervens et al., 2011; Lin et al., 2014; Xing et al., 2019). As wall loss of organic vapors is recognized to be non-negligible in determining SOA production in chamber experiments, wall loss-corrected SOA production has recently been applied in model parameterization (Cappa et al., 2016; La et al., 2016). However, discrepancies still exist between simulated and observed SOA budgets (Hallquist et al., 2009; Shrivastava et al., 2017; Kelly et al., 2018). This might further induce potential uncertainties in the estimation of global

climate forcing because SOA is capable of scattering and absorbing radiation and to influence the amount of cloud condensation nuclei (Carslaw et al., 2013; Shrivastava et al., 2017).

The urge to better reproduce observed ambient SOA concentration by models has motivated the related research that attempted to distinguish missed SOA sources and unknown SOA formation mechanism (Li et al., 2017b; Couvidat et al., 2018; Xu et al., 2018). Exploring SOA formation potential and mechanism from various anthropogenic and biogenic VOCs (BVOCs) have been the focus of numerous laboratory experiments. Their contribution to total SOA budget has often been separately parameterized in models (Kelly et al., 2018; Jiang et al., 2019). Globally, the concentration of BVOCs emitted from terrestrial ecosystems was estimated to be 1000 Tg yr^{-1} (Guenther et al., 2012), which was roughly 8 times higher than those from anthropogenic sources (127 Tg yr^{-1}) (Glasius and Goldstein, 2016). BVOCs, including isoprene (C_5H_8, ~ 50%), monoterpenes ($C_{10}H_{16}$, ~ 15%) and sesquiterpenes ($C_{15}H_{24}$, ~ 3%) are important SOA formation precursors owing to their large emission and high reactivity towards atmospheric oxidants (e.g. hydroxyl radical (·OH), ozone, nitrate radical (NO_3·)) (Guenther et al., 2012; Jaoui et al., 2013; Ehn et al., 2014; Ng et al., 2017). Consequently, a large fraction of the global SOA (67% - 95%) is estimated to derive from biogenic sources (Farina et al., 2010; Hodzic et al., 2016; Kelly et al., 2018).

Separating the anthropogenic SOA from the biogenic contribution in SOA formation is effective to improve models performance but is not sufficient to capture all human-induced SOA formation (Hodzic et al., 2016; Kelly et al., 2018; Jiang et al., 2019). Recently, anthropogenic pollutants have been suggested to indirectly participate in biogenic SOA formation through anthropogenic-biogenic interactions (Hoyle et al., 2011; Xu et al., 2015b; Zhang et al., 2018; Zhao et al., 2018b; Wu et al., 2020). For

example, about 80% of biogenic SOA in East Asia was predicted to be influenced by anthropogenic emissions, while in regions with less anthropogenic emissions, like eastern US, this value is larger than 50% (Carlton et al., 2010; Matsui et al., 2014). This 'anthropogenic enhancement' effect on biogenic SOA formation indicates that though naturally emitted BVOCs dominate over anthropogenic VOCs and cannot be controlled directly, biogenic SOA can somewhat be controlled by limiting manmade pollutants through air quality control policies (Edwards et al., 2017; Marais et al., 2017).

Nitrogen dioxides (NOx = NO + NO_2), sulfur dioxide (SO_2), ammonia (NH_3), and primary particles are prevalent anthropogenic pollutants. Traditional air quality policies target at controlling their emissions for the purpose of mitigating the formation of secondary inorganic aerosols and associated environmental issues (Wang et al., 2013; Liu et al., 2019). Though the global SO_2 emission has largely decreased in recent decades, the emissions of NOx and NH_3 show increasing trends (Warner et al., 2017; Hoesly et al., 2018) and POA is still a significant component of polluted air in some regions (Zhang et al., 2015a; Li et al., 2017a; Jiang et al., 2019). When anthropogenic emissions enriched air mass is transported to areas with substantial BVOCs emissions, anthropogenic-biogenic interactions happen to perturb the BVOCs oxidation and thus corresponding SOA formation processes (Zhao et al., 2018b). The key goal of numerous recent research has therefore been to determine the mechanisms of the anthropogenic-biogenic interactions (Ye et al., 2018; Slade et al., 2019), and the extent to which biogenic SOA can be controlled by eliminating predominant anthropogenic species such as NOx, SO_2, NH_3 and some primary aerosols (Carlton et al., 2010; Edwards et al., 2017). The ultimate aim is to achieve more reasonable parameterization of SOA budgets and effects, to evaluate models and to formulate more effective policies to alleviate air quality deterioration triggered by aerosol particles (Hettiyadura et al.,

2019; Wu et al., 2020).

This review seeks to summarize the recent progress in the research related to the interaction between anthropogenic species and natural biogenic emissions. Section 2 reviews effects of NOx on biogenic SOA formation during daytime and nighttime. Section 3 describes the role of anthropogenic aerosol gas-particle partition and the particle-phase reactions. Section 4 contains the photooxidation and ozonolysis of BVOCs modified by SO_2. Biogenic SOA formation and aging in the presence of ammonia/amines are presented in section 5 and recent field studies focusing on anthropogenic-biogenic interactions in China are discussed in section 6. The final section is the summary of this review and outlook about future studies toward anthropogenic-biogenic interactions. Overall, this review tries to comprehensively summarize the recent advances in understanding the influence of anthropogenic emissions on biogenic SOA formation, to enlighten future observational and modeling studies in regions influenced both by anthropogenic and natural emissions, and to aid in the better formulation of pollution control strategies.

2. Effects of NOx on biogenic SOA formation during daytime and nighttime

The majority of NOx in the atmosphere comes from combustion-related human activities, including transportation, industrial boilers, power plants, home heating and municipal incineration (von Schneidemesser et al., 2015). The global emission of NOx from these anthropogenic sources was estimated to be approximately 130 Tg (NO_2) for the year 2014 (Hoesly et al., 2018). The close linkage between NOx and biogenic SOA formation is reflected in its ability to alter SOA formation mechanism, composition and yield via affecting the gas-phase chemistry, gas-particle partition and particle-phase reactions, both during daytime and nighttime (Ma et al., 2012; Rollins et al., 2012).

144 ***2.1 BVOCs photooxidation and SOA formation***

145 BVOCs oxidation during daylight hours is dominated by ·OH (Ziemann and
146 Atkinson, 2012). The initial addition or H-abstraction reaction between ·OH and
147 BVOCs results in alkyl-type radicals (R·), most of which react rapidly with O_2, leading
148 to organic peroxy radicals (RO_2·) (Atkinson, 2000). The general schematic of
149 RO_2· chemistry in SOA formation is summarized in Fig. 1. The influence of NOx is
150 derived from its alteration on the fate of RO_2·, which can either react with RO_2·,
151 hydroperoxy radicals (HO_2·) or NOx under certain conditions. The different
152 RO_2· branches determine the distribution of oxidized products. For example, the
153 reaction between RO_2· and HO_2· often produces hydroperoxides with low-volatility,
154 RO_2· self-reaction or reactions with other RO_2· form alcohol or carbonyls and the RO_2·
155 + NO reaction usually leads to organic nitrates as well as alkoxy radicals (RO·) that
156 either undergo fragmentation or isomerization to form more volatile products (Ziemann
157 and Atkinson, 2012; Sarrafzadeh et al., 2016). Since the fate of RO_2· is highly related
158 to the relative concentration of NOx and VOCs in the urban atmosphere, laboratory
159 chamber experiments often use the ratio of initial BVOCs and NOx concentration
160 ($[BVOC]_0/[NOx]_0$ or $[NOx]_0/[BVOC]_0$) to restrict RO_2· chemistry from the
161 interpretation of NOx effects on new particle formation and SOA yields (Pandis et al.,
162 1991; Presto et al., 2005; Kim et al., 2012; Wildt et al., 2014; Xu et al., 2014; Stirnweis
163 et al., 2017). It should be noted that attention must be paid to evaluate the O_3-induced
164 loss of BVOCs in the photooxidation system because O_3 production and its effect would
165 also vary with the $[BVOC]_0/[NOx]_0$ ratio, the relative rates of ozonolysis and ·OH
166 oxidation and some other reaction conditions (Griffin et al., 1999). For biogenic SOA
167 formation in the presence of NOx listed in Table 1, the completely dominant role of ·OH
168 oxidation in BVOC loss was estimated and thus O_3 generation would not influence the

NOx-dependent SOA yield.

The SOA yield is defined as the formed SOA mass concentration (ΔM, μg m^{-3}) relative to the consumed parent hydrocarbon (ΔBVOC, μg m^{-3}). The impact of NOx on SOA yields depends on the SOA mass production and is also parent hydrocarbon-specific (Table 1). For isoprene, the most abundant BVOC in the atmosphere (Kroll et al., 2006; Chan et al., 2010; Xu et al., 2014), the pathways of its reaction with $RO_2\cdot$ under low and high NOx conditions were quite different (Fig. 2). Chamber studies have generally evidenced higher SOA yields at lower $[NOx]_0/[isoprene]_0$ ratios, and most of these studies suggested that SOA yields first increase and then decrease with the increasing $[NOx]_0/[isoprene]_0$ ratios (Dommen et al., 2006; Kroll et al., 2006; King et al., 2010; Xu et al., 2014; Liu et al., 2016). The decrease of SOA yield with increasing NOx, more precisely with increasing NO, was generally explained by the dominated $RO_2\cdot$ + NO reactions over $RO_2\cdot$ + $HO_2\cdot$ reactions, with the former reaction producing more volatile products (such as organic nitrates) than the latter (hydroperoxides) (Kroll et al., 2006; Xu et al., 2014). Kroll et al. (2006) considered that the decline of NO/$HO_2\cdot$ ratio that may lead to a switch from high-NOx to low-NOx conditions over the experimental process might result in the complex SOA yield dependence under lower NOx condition ($[NOx]_0/[isoprene]_0 < 4.4$). Xu et al. (2014) also observed the similar nonlinear variation of aerosol volatility and oxidation state level with $[NO]_0/[isoprene]_0$ ratio (0 - 7.3) as the SOA yield. They proposed that the presence of NO enhanced the formation of methacrolein, the first generation product, whose further oxidation forms SOA-forming organics efficiently (Surratt et al., 2010), leading to increased SOA yield and decreased aerosol volatility when $[NO]_0/[isoprene]_0$ was lower than 3. In a more recent study focusing on a lower $[NO]_0/[isoprene]_0$ range (0 - 2), the SOA yield was nearly constant when the $[NO]_0/[isoprene]_0$ ratio was lower than ~ 0.38 (Liu et al.,

2016). After this NO threshold level, the SOA yield decreased from 12% to 3% with further increase of NOx, accompanied by the decrease of more highly oxygenated organic nitrates. These observations were explained by the suppression of NO on hydroxy hydroperoxide that acts as the source of $C_5H_{11}O_6$ peroxyl radical and thus lower the production of both second-generation multifunctional peroxides and multifunctional organic nitrates (Fig. 2). Similarly, with the composition analysis of isoprene SOA formed under low NOx in laboratory and aerosol samples collected from the isoprene-rich southeastern US environment, the none-IEPOX pathway under low NOx condition was also suggested to contribute to notable highly oxidized compounds and SOA mass (Riva et al., 2016c).

Note that though similar trends of isoprene SOA yield response to NOx level were observed among different studies, the critical $[NOx]_0/[isoprene]_0$ points for the transition role of NOx are quite different (e.g. 4.4 (Kroll et al., 2006), 0.38 (Liu et al., 2016), and ~3 (Xu et al., 2014)). It has been shown that even under the same $[NOx]_0/[isoprene]_0$ ratios, the fate of $RO_2\cdot$ radicals that are responsible for SOA formation can be quite different (Ng et al., 2007a). Recent studies suggested that the composition of NOx itself is also a candidate for altering SOA formation pathways (Chan et al., 2010; Surratt et al., 2010). For example, oligoesters of dihydroxycarboxylic acids and hydroxynitrooxycarboxylic acids from isoprene photooxidation increased with increasing NO_2/NO ratios (Chan et al., 2010). More recent studies showed that SOA yields under high NOx conditions can be as high as those under low-NOx conditions because the $NO_2 + RO_2\cdot$ reaction can potentially yield substantial SOA mass (e.g. hydroxymethylmethyl-α-lactone, methacrylic acid) via the subsequent oxidation of methacryloylperoxynitrate, which is favorably formed from methacrolein (first-generation products of isoprene photooxidation) oxidation under

high NO_2/NO ratios (Fig. 2) (Chan et al., 2010; Surratt et al., 2010; Lin et al., 2012; Lin et al., 2013b; Pye et al., 2013; Nguyen et al., 2015). Besides NO_2/NO ratios, the ·OH precursors, such as HONO that strongly suppresses ISOPOOH chemistry and thus the formation of the second-generation organic nitrates, the chamber operation mode (flow or batch mode) and some other reaction conditions (e.g. seed particles) are potential factors to induce the differences in threshold $[NOx]_0$/$[isoprene]_0$ values and warrant further studies for more accurate model parametrization (Kroll et al., 2005; Xu et al., 2014; Liu et al., 2016; Shrivastava et al., 2017).

The effects of NOx on SOA formation from the photooxidation of monoterpenes, especially *α*-pinene, *β*-pinene and limonene have also been characterized by chamber studies (Pandis et al., 1991; Zhang et al., 1992; Ng et al., 2007b; Eddingsaas et al., 2012; Kim et al., 2012; Wildt et al., 2014; Sarrafzadeh et al., 2016; Stirnweis et al., 2017; Zhao et al., 2018b). As summarized in Table 1, SOA yields are generally higher at low NOx than at high NOx conditions when monoterpene ozonolysis is negligible. Besides the perturbation of NOx on RO_2· chemistry, recent studies found that NOx influence the SOA yield by altering the ·OH cycle and new particle formation (NPF) (Wildt et al., 2014; Sarrafzadeh et al., 2016; Zhao et al., 2018b). Using realistic BVOCs mixture emitted directly by plants, Wildt et al. (2014) found that NPF was suppressed at high NOx conditions ($[BVOC]_0/[NOx]_0 < 7$, $[NOx]_0 > 23$ ppb). The self-reaction of higher generation peroxy radical-like intermediates and their reaction with NO commonly limited the rate of new particle formation. More recently, the study focusing on *β*-pinene photooxidation showed that at low NOx conditions ($[\beta\text{-pinene}]_0/[NOx]_0 >$ 10 ppbC ppb^{-1}), the increase of ·OH radical through NO + HO_2· → NO_2 + ·OH reaction was responsible for the increase of SOA yield with the increase of NOx (Sarrafzadeh et al., 2016). It was also evidenced that the ratio of NO/NO_2 was correlated with the ·OH

244 cycle and, thus, probably influenced SOA formation. At high NOx conditions ([β-
245 pinene]$_0$/[NOx]$_0$ = ~ 10 to ~ 2.6 ppbC ppb^{-1}), the decrease of SOA yield with NOx was
246 attributed to NOx-triggered suppression of low volatility products (such as
247 hydroperoxides) that participated in NPF. The restrained NPF would further result in
248 limited particle surface for the condensation of low volatile species. Similarly, the
249 suppression effect of NOx on NPF has been evidenced during the photooxidation of α-
250 pinene and limonene (Zhao et al., 2018b).

251 Sesquiterpenes on a reacted mass basis have much higher SOA formation potential
252 than isoprene and monoterpenes due to their higher molecular weight and reactivity
253 (Lee et al., 2006; Jaoui et al., 2013). As opposed to NOx effects on SOA formation
254 from isoprene and monoterpenes photooxidation, SOA formed from longifolene,
255 aromadendren and β-caryophyllene photooxidation under high NOx conditions
256 substantially exceeds that under low NOx conditions (Ng et al., 2007b; Tasoglou and
257 Pandis, 2015). The formation of less-volatility products (e.g. large hydroxycarbonyls,
258 multifunctional species) via isomerization instead of decomposition of large RO· and
259 the relatively low volatile organic nitrates were proposed to be responsible for this
260 positive NOx effect. However, SOA yields from β-caryophyllene in the works of
261 Griffin et al. (1999) and Alfarra et al. (2012) were less dependent on [NOx]$_0$/[BVOC]$_0$
262 ratios, probably due to the interference of other experimental conditions (e.g. OH
263 precursors, the initial BVOC mixing ratios). Clearly, if the positive NOx effect on SOA
264 formation observed by Ng et al. (2007b) can be extended to other sesquiterpenes, the
265 contribution of sesquiterpenes to SOA in NOx-polluted air may be much higher (Ng et
266 al., 2007b). A recent modeling study in the southeastern US showed underestimated
267 SOA formation from monoterpenes and sesquiterpenes and argued that anthropogenic
268 emissions would exert complex influences on biogenic SOA formation (Xu et al., 2018).

Considering that the studies on NOx effects only target a limited number of sesquiterpenes, a thorough evaluation of the effect of NOx on the photooxidation of a complete suite of sesquiterpenes is necessary for a better constrain of their oxidation and contribution to ambient SOA.

2.2 Biogenic SOA formation under dark conditions

The night time biogenic SOA formation in the atmosphere is sensitive to NOx levels due to the changed radical (e.g. $RO_2\cdot$, $HO_2\cdot$, $NO_3\cdot$) chemistry and the oxidation capacity (Brown and Stutz, 2012; Ng et al., 2017). While ·OH dominates daytime BVOCs oxidation, $NO_3\cdot$ that is mainly produced via the reaction between O_3 and NO_2 becomes one of the main oxidants at night (Fig. 1) (Wayne et al., 1991; Rollins et al., 2012; Edwards et al., 2017). The unsaturated and non-aromatic nature of BVOCs makes them particularly susceptible to the oxidation by $NO_3\cdot$ and O_3 (Atkinson and Arey, 1998; Ayres et al., 2015). The competition between these two BVOCs sinks is highly associated with the NOx level and composition because of the loss of $NO_3\cdot$ through its reaction of NO and a decrease of its production through the reaction of NO_2 and O_3 as O_3 is decreased by the reaction of O_3 and NO (Rollins et al., 2012; Qin et al., 2018b; Wang et al., 2020a). The oxidation of BVOCs by $NO_3\cdot$ occurs mainly via the addition of $NO_3\cdot$ to the unsaturated bonds (another pathway is hydrogen-abstraction favored for aldehydic species), forming alkyl radicals that would either lose NO_2 to form epoxides or further react with O_2 to form $RO_2\cdot$ (Fig. 1) (Ng et al., 2017; Fouqueau et al., 2020). $RO_2\cdot$ would isomerize or react with $HO_2\cdot$, $NO_3\cdot$ or $RO_2\cdot$ to form various products such as organic nitrates that potentially generate SOA. $NO_3\cdot$-BVOCs chemistry is thus regarded as a prominent candidate for the generation of biogenic SOA and organic nitrates that are correlated with anthropogenic tracers (Fry et al., 2009; Kiendler-Scharr et al., 2016; Huang et al., 2019).

Such correlations have been evidenced in recent field observations around the world (Rollins et al., 2012; Brown et al., 2013; Kiendler-Scharr et al., 2016; Edwards et al., 2017; Fry et al., 2018; Yu et al., 2019). In a rural area in southwest Germany, the contribution of organic nitrates to the increase of newly formed particles after sunset was observed to be 18-25%. Considering both high BVOCs and NOx emission in this area, the reactions between $NO_3\cdot$ and BVOCs, especially monoterpenes, are responsible for organic nitrates and SOA formation (Huang et al., 2019). In some forest regions of the US, the concentration of organic nitrates was found to peak at night and its contribution to the total organic aerosol was up to 40% in Bakersfield due to nighttime oxidation of BVOCs by $NO_3\cdot$ (Rollins et al., 2012; Fry et al., 2013; Xu et al., 2015a). A substantial contribution of organic nitrates that are formed via nocturnal $NO_3\cdot$-BVOCs chemistry to particulate organic mass has also been observed in Europe and China (Kiendler-Scharr et al., 2016; Yu et al., 2019). Interestingly, the observation in the forest region of western US showed that the concentration of nighttime aerosol organic nitrates was positively correlated with the product of the mixing ratios of NO_2 and O_3 instead of that of O_3 alone (Fry et al., 2013). This indicates that $NO_3\cdot$-initiated oxidation of monoterpenes is related to NOx level and is an important source of particle-phase organic nitrates at night.

The SOA formation potential of various BVOCs oxidized by $NO_3\cdot$ has been investigated in many chamber studies (Ng et al. (2017) and references therein). The reported SOA yields vary among different BVOCs, from nearly 0 for α-pinene, to 0.12 for isoprene, 0.33-0.44 for β-pinene, 0.44-0.57 for limonene and to 0.86 for β-caryophyllene at an atmospheric relevant aerosol mass loading of 10 μg m^{-3} (Fry et al., 2014). Except for α-pinene, these yield values are much higher than those from the ozonolysis of corresponding BVOCs (Song et al., 2007; Hessberg et al., 2009; Saathoff

et al., 2009; Tasoglou and Pandis, 2015). The relative importance of $NO_3\cdot$ oxidation versus O_3 is connected with the ratio of $NO_3\cdot$ production to BVOCs ozonolysis (Griffin et al., 1999). Considering for example 10 ppt $NO_3\cdot$ and 30 ppb O_3, the oxidation of these monoterpenes by $NO_3\cdot$ proceeds 20-90 times faster than their ozonolysis, due to the much higher rate constants of the former reactions (Fry et al., 2014). The accelerated BVOCs consumption by $NO_3\cdot$ here is somewhat in consistence with the field observations that found $NO_3\cdot$ + monoterpenes chemistry to be a significant nighttime aerosol source in regions with high NOx level.

While most chamber studies directly investigated $NO_3\cdot$-induced SOA under purified $NO_3\cdot$ conditions (Griffin et al., 1999; Hallquist et al., 1999; Fry et al., 2014), some recent works have examined the biogenic SOA formation in the presence of Ox (O_3 + NO_2) (Table 2) (Presto et al., 2005; Perraud et al., 2012; Draper et al., 2015; Chen et al., 2017; Xu et al., 2020). The effects of NO_2 on the dark ozonolysis of β-pinene, Δ^3-carene, and limonene were examined by keeping O_3 mixing ratio constant while varying NO_2 mixing ratios ($[O_3]_0/[NO_2]_0$ = 2-0.5, $[NO_2]_0/[BVOCs]_0$ = 0.5-1). It was found that for β-pinene and Δ^3-carene, SOA yields were comparable over the range of oxidation conditions. The increase of limonene SOA yield with increasing NO_2 mixing ratio was observed and attributed to the increased fraction of oligomers and multifunctional organic nitrates in SOA through $NO_3\cdot$ chemistry (Draper et al., 2015). More recently, γ-terpinene SOA yield, as well as the contribution of organic nitrates to particle mass both increased with increasing NO_2 levels ($[NO_2]_0/[O_3]_0$ = 0-0.7, $[NO_2]_0/[\gamma\text{-terpinene}]_0$ = 0-3)) due to the change from O_3-dominanted to $NO_3\cdot$-dominanted γ-terpinene oxidation that yield organic nitrates as significant SOA components (Xu et al., 2020). Among the studied monoterpenes, α-pinene exhibited quite different NO_2 response during ozonolysis. Several studies consistently found that

SOA yields, as well as particle number concentrations decreased with increasing NOx (Presto et al., 2005; Nøjgaard et al., 2006; Perraud et al., 2012; Draper et al., 2015). This is expected because the SOA yield from α-pinene ozonolysis is higher than that from $NO_3\cdot$ oxidation, the latter process forming organic nitrates that have relative high volatility and thus, inefficient to nucleate (Perraud et al., 2012). In the real atmosphere, the good correlation between Ox and biogenic SOA tracers was also observed in the field campaign carried out in the Pearl River Delta, South China (Zhang et al., 2019b). With the elevation of Ox in the atmosphere, more observations focusing on the linkage between Ox and biogenic SOA are necessary but still limited. Altogether, these studies suggest that models should carefully handle the Ox effects on nocturnal SOA formation by capturing the detailed spatial distribution of BVOCs and Ox in order to reduce the uncertainty in the estimation of regional or global SOA budget (Fry et al., 2014; Fry et al., 2018).

3. Effects of anthropogenic aerosol on gas-particle partitioning and particle-phase reactions in SOA formation

Human activities induce a variety of organic or inorganic particles, both of which can be primarily emitted (e.g. soot, primary organic aerosol (POA) from fossil fuel, biofuel, and agricultural combustion) or secondarily formed (e.g. SOA-derived from anthropogenic VOCs, sulfate, nitrate and ammonium associated with gaseous SO_2, NOx and NH_3) in the atmosphere (Goldstein et al., 2009; Wang et al., 2020b). Interactions then arise between anthropogenic aerosol and biogenic SOA formation due to the potential influences of anthropogenic aerosol on gas-particle partitioning of BVOCs oxidation products and particle-phase reactions.

3.1 Gas-particle partition

BVOCs oxidation could form semi-volatile organic compounds (SVOCs) that undergo partition between the gas- and particle- phases. The SOA yield that is defined as the ratio of the organic aerosol mass concentration to the BVOCs consumption, can be modeled by the gas-particle partitioning absorption model (Pankow, 1994b; Odum et al., 1996),

$$Y = \frac{\Delta M_0}{\Delta[BVOC]} = M_0 \sum_i \left(\frac{\alpha_i K_{om,i}}{1 + K_{om,i} M_0}\right) \quad (1)$$

where α_i is the mass-based stoichiometric coefficient of product i, $K_{om,i}$ ($m^3\ \mu g^{-1}$) is the partitioning coefficient of the gas–particle partitioning defined by the ratio of absorption equilibrium constant ($K_{p,i}$) to the mass fraction of species i in the aerosol-phase (f_{om}) (Pankow, 1994b,a; Odum et al., 1996).

$K_{p,i}$ can be calculated by the following equation: (Donahue et al., 2006; Zhang et al., 2015b)

$$K_{p,i} = \frac{1}{C_i^*} = \frac{C_i^{aer}}{C_i^{vap} M_0} \quad (2)$$

where C_i^* is the effective saturation concentration of species i, C_i^{aer} and C_i^{vap} are the mass concentrations of component i in the aerosol-phase and gas-phase, respectively. With the assumption that SOA formed from BVOCs oxidation can be well-mixed with preexisting organic aerosol, eq (2) indicates that in cases where the absorbing organic mass is present, some fraction of SVOCs could partition into the particle-phase even if their gas-phase concentration is lower than their saturation vapor pressure (Kroll and Seinfeld, 2008). Preexisting organic seed aerosols make SOA to be diluted and C_i^{aer} would decrease when they mix with each other. The decreased activity for species i restrains its evaporation from the particle-phase to the gas-phase in accordance to Raoult's Law. The partitioning equilibrium is therefore shifted to the condensed-phase, increasing SOA mass formation and, thus, the SOA yield.

Anthropogenic POA makes up a significant fraction of total OA in the atmosphere, especially under severe air pollution in winter (Li et al., 2017a; Zhang et al., 2017a). Based on the gas-particle partition mechanism, it has been predicted that biogenic SOA would be largely enhanced by POA emission (Heald et al., 2008; Hoyle et al., 2009; Carlton et al., 2010; Carlton et al., 2018). Some recent studies argued that the enhanced biogenic SOA formation would be overestimated probably because the assumption of well-mixed organic aerosol-phase between POA and SOA in models is not always the case for the real atmosphere (Loza et al., 2013; Robinson et al., 2015), though this assumption is reasonable in SOA formation because most of the SOA components are oxygenated polar organic species that are miscible with one another (Song et al., 2007). Ambient POA contains a large fraction of hydrophobic non-polar species and phase-separation often occurs. The existence of such morphologies would affect the gas-particle partition of SVOCs, therefore affecting SOA formation and its optical properties (Song et al., 2007; George et al., 2015).

Several chamber experiments were conducted to examine the mixing behavior of POA and biogenic SOA and thus, the applicability of the single-phase assumption in models (Robinson et al., 2013). For example, using dioctyl phthalate (DOP) and lubricating oil as surrogates of urban hydrophobic POA, the SOA mass from the α-pinene ozonolysis (can also be applied to other BVOCs) was insensitive to these seed aerosols (Fig. 3 (a)) (Song et al., 2007). Implying the no seed parameters and the sum of seed and aerosol masses as M_0, the seeded SOA mass was 13-44% higher than the observed value and phase separation could therefore appear. This is reasonable because multifunctional species formed from α-pinene ozonolysis have polar properties, which are exactly opposite to those of DOP and lubricating oil components. The layered phase between α-pinene SOA and DOP POA was further confirmed by a single-particle mass

spectrometer that is able to distinguish whether SOA and DOP were homogeneously mixed by changing laser power (Vaden et al., 2010). The high MS intensity of the surface material at low laser power instead of the constant relative MS intensities with changing laser powers was observed, supporting the phase-separation (Fig.3 (b)). On the contrary, the time evolution of the aerodynamic vacuum diameter of diesel POA (DL) and α-pinene SOA mixture showed the transformation of bimodal distribution to single modal distribution (Fig. 3 (c)), indicating the formation of a single-phase between α-pinene SOA and DL (Asa-Awuku et al., 2009). SOA from β-caryophyllene ozonolysis also formed a well-mixed phase with DL, but these SOA and α-pinene SOA were immiscible with motor oil and diesel fuel POA. This study supports the use of the single-phase assumption in atmospheric models because diesel exhaust POA is the most atmospherically relevant case. Anthropogenic SOA formed from the photooxidation of aromatic hydrocarbons enhanced SOA formation from α-pinene oxidation, indicating that the interaction between these different types of SOA formed an ideal mixing state (Hildebrandt et al., 2011; Emanuelsson et al., 2013; Robinson et al., 2013). Clearly, the polarity of anthropogenic OA reflects its mixing behavior with biogenic SOA. The incorporation of the distribution of different types of anthropogenic OA in the real atmosphere into regional or global models is crucial in evaluating the effects of anthropogenic OA on biogenic SOA formation.

3.2 Particle-phase reactions

Particle-phase reactions including both heterogeneous and multiphase reactions are significant in biogenic SOA formation due to their ability to form lower volatility compounds (Kroll and Seinfeld, 2008). Reactive uptake of gaseous products via accretion reactions, such as hydration, polymerization, esterification, hemiacetal/acetal formation, and aldol condensation are often acid catalyzed (Fig. 4) (Jang et al., 2002;

442 Hallquist et al., 2009; Darer et al., 2011; Ziemann and Atkinson, 2012; Couvidat et al.,
443 2018). Isomerization of highly reactive species in the presence of acidic sulfate particles
444 is also a potential pathway to induce acid-catalyzed enhancement on SOA formation
445 (Fig. 4 (h)) (Lin et al., 2012; Iinuma et al., 2013). Combining field measurements of
446 concentrations of water-soluble ions (K^+, Ca^{2+}, Mg^{2+}, NO_3^-, NH_4^+, Na^+, SO_4^{2-}, Cl^-) and
447 indirect estimation (e.g. thermodynamic equilibrium models and ion balance method),
448 the acidic characteristic of ambient particles was determined. For instance, the mean
449 pH values in urban Beijing and rural Gucheng of China were determined to be 5.0 and
450 5.3, respectively (Hennigan et al., 2015; Shi et al., 2017; Chi et al., 2018). More acidic
451 particles (pH ranges from 0 to 2) were observed in southeastern US (Guo et al., 2015;
452 Weber et al., 2016). Sources of particle acidity have been resolved to be secondary
453 nitrate and sulfate associated with gaseous NOx, SO_2 and ammonia, coal combustion,
454 vehicle exhaust, and mineral dust (Weber et al., 2016; Shi et al., 2017). Thus, human
455 activities link to biogenic SOA formation via these particle-phase reactions that are
456 correlated with particle acidity (Surratt et al., 2010; Qin et al., 2018a).

457 Numerous laboratory experiments were conducted with acidic seed particles to
458 investigate the acidity effects on biogenic SOA formation. Improved SOA yields in the
459 presence of acidic seed have been observed for a series of BVOCs due to the reactive
460 uptake of the oxidation products (Gao et al., 2004; Iinuma et al., 2004; Offenberg et al.,
461 2009; Han et al., 2016; Riva et al., 2016a), but this dependence is not always the case
462 for all BVOCs due to varied experimental conditions. Taking α-pinene as an example,
463 while organic carbon (OC) from its pure ozonolysis in the presence of sulfuric acid was
464 40% higher than that of ammonium sulfate (Iinuma et al., 2004), another ozonolysis
465 study under low-NO*x* conditions found a negligible effect of increasing particle acidity
466 on α-pinene SOA formation (Kristensen et al., 2014). In α-pinene photooxidation, the

467 SOA yield increased nearly linearly with particle acidity under high-NO*x* conditions,
468 significantly different from the negligible acidity effect under low-NO*x* conditions
469 (Han et al., 2016). In another study, it was observed that seed acidity only enhanced
470 particle yields under high-NO condition but not under high-NO_2 condition because
471 increased nitric acid and peroxyacyl nitrates in the latter case would make the aerosol
472 acidic enough even in the presence of neutral seeds (Eddingsaas et al., 2012). These
473 inconsistent results suggest that the effect of acidity on biogenic SOA formation might
474 be mediated by other conditions such as initial hydrocarbon concentration, oxidant type,
475 and NOx levels. Exploring the effect of acidity on biogenic SOA formation under more
476 atmospheric relevant conditions is needed.

477 Isoprene as the most abundant biogenic hydrocarbon and largest SOA source, has
478 gained particular concern (Hallquist et al., 2009). Collectively, acidic seeds enhance
479 isoprene SOA yields from both photooxidation and ozonolysis through acid-catalyzed
480 particle-phase reactions (Jang et al., 2002; Czoschke et al., 2003; Surratt et al., 2007;
481 Zhang et al., 2011; Riva et al., 2016a). This was evidenced by increased 2-methyltetrol,
482 organosulfates, and high molecular weight oligomers with aerosol acidity. Further
483 studies underlined the importance of reactive uptake of isoprene epoxydiols (IEPOX)
484 that are formed through isoprene photooxidation under low NOx conditions (Fig. 2)
485 (Lin et al., 2012; Riva et al., 2016b). The acid-catalyzed nucleophilic addition of sulfate
486 to the epoxide ring of IEPOX contributed substantially to SOA formation (Fig. 4 (f))
487 (Surratt et al., 2010; Darer et al., 2011; Gaston et al., 2014). Organosulfates formed
488 through this low NOx channel accounted for ~ 97%, ~ 55% and 62% - 83% of SOA
489 mass in the Amazon, the southeastern US, and southwestern China, respectively (Qin
490 et al., 2018a; Yee et al., 2020). It has been shown that the reaction probability of IEPOX
491 on ammonium bisulfate was more than 500 times greater than on ammonium sulfate

and low NOx isoprene SOA yield increased from 1.3% in the presence of neutral particle to 28.6% in the presence of acidic particles (Surratt et al., 2010; Gaston et al., 2014). However, the reactive uptake of IEPOX was also observed to increase the OA mass when base hydrated ammonium sulfate was used (Nguyen et al., 2014). Hydrated seed particles here promoted not only the dissolution of water-soluble compounds but also hydrolysis reactions in the aqueous-phase.

The weak correlations between particle acidity and IEPOX-derived SOA here are somewhat consistent with field observations (Budisulistiorini et al., 2013; Worton et al., 2013; Budisulistiorini et al., 2015; Xu et al., 2015b). For example, in southwestern and eastern China and the southeastern US, isoprene SOA was found to be more strongly correlated with sulfate than with particle acidity or water mass concentration, partially because the surface area provided by sulfate particles promoted IEPOX reactive uptake and sulfate as a nucleophile and/or the salting-in effect accelerated the ring-opening reactions of IEPOX (Xu et al., 2015b; Rattanavaraha et al., 2017; Zhang et al., 2017c; Qin et al., 2018a). The insignificant correlation of IEPOX SOA with pH was ascribed to the small pH range and the regional transportation caused gap between calculated and the real particle pH at the time/site where acidity-dependent chemistry occurred (Yee et al., 2020). With a more detailed interpretation of the observed relationship between isoprene SOA tracers and pH, the particle acidity was found to negatively correlate with the ratio of 2-methyltetrols to C5-alkene triols (IEPOX pathway in Fig. 2), indicating that the formation of C5-alkene triols was favored with increasing particle acidity (Yee et al., 2020). However, it might be easy to misinterpret the effect of particle acidity and water on isoprene SOA formation because they are driven by sulfate (Xu et al., 2015b). The much more complex atmospheric environments than experimental conditions may partially lead to the gap between these

two kinds of studies. The difference in particle acidity in laboratory experiments and real atmosphere, the accurate manner and degree to which relative humidity and the liquid water content, seed particle composition, and acidity influence isoprene and other BVOCs-derived SOA formation remain elusive, and deserve further systemically exploration under more atmospherically relevant conditions (Lin et al., 2013a; Budisulistiorini et al., 2015; Riva et al., 2016b; Faust et al., 2017; Stirnweis et al., 2017).

Dicarboxylic acids (DCA) with the predominance of oxalic acid are major components of atmospheric organic aerosols. They have gained considerable attention in recent years owing to their contribution to organic aerosol budget via SOA formation and the potential impacts on climate via changing the solar radiation and acting as cloud condensation nuclei (Bikkina et al., 2014; Kawamura and Bikkina, 2016). While their emission from primary sources such as biomass burning and vehicle exhausts, cooking and natural marine sources are relatively low, those in the atmosphere originate largely from the photochemistry of biogenic unsaturated fatty acids and VOCs such as isoprene and intermediates (Lim et al., 2005; Carlton et al., 2007; Ervens et al., 2011). These processes are discussed to help understand how anthropogenic factors would influence DCA SOA formation.

Unsaturated fatty acids such as oleic acid are rich in marine phytoplankton and terrestrial higher plant leave (Ho et al., 2010). For SOA formation from unsaturated fatty acids, the ozonolysis of oleic acid particles under dry conditions showed a pronounced mass loss of oleic acid particles due to the evaporation of volatile oxidation products such as nonanal (Lee et al., 2012). However, azelaic acid in the particulate phase can further generate low molecular weight DCA such as oxalic acid, which is a major class of SOA. In marine regions, azelaic acid and DCA concentrations were higher in more biologically influenced aerosols than in less biologically influenced ones,

suggesting the contribution of biogenic unsaturated fatty acids to DCA formation (Bikkina et al., 2014).

The ability of isoprene as a precursor of DCA, especially oxalic acid has been evidenced in various regions. In marine regions, isoprene was proposed to be one source of DCA through aqueous-phase reactions (Bikkina et al., 2014; Bikkina et al., 2015). Pyruvic and glyoxylic acids and methylglyoxal in the aerosol-phase are key precursors for the final formation of oxalic acid. In continental regions, oxalic acid and glyoxylic acid that derived from glyoxal and methylglyoxal (important isoprene oxidation products) oxidation were observed to have a robust linear correlation and also well correlated with sulfate, indicating that oxalic acid may be largely produced by aqueous phase oxidation of glyoxylic acid in aerosols (Yu et al., 2005; Fu et al., 2008; Wang et al., 2012). More recently, a field observation in Xi'an, China, focusing on the formation mechanism of SOA on dust surfaces investigated the concentrations and compositions of DCA during the dust storm episodes (Wang et al., 2015). According to the strong correlation of oxalic acid with NO_3^-, $Ca(NO_3)_2$ that strongly absorbs water vapor was proposed to be produced via the heterogeneous reaction of nitric acid and/or nitrogen oxides with dust (Wang et al., 2015). Gas-phase water-soluble organic precursors (e.g., glyoxal and methylglyoxal) that partitioned into the aqueous-phase on the surface of dust aerosols can be subsequently oxidized into oxalic acid and thus contributed to SOA formation. It seems that liquid water in particles favors organic acid formation (Lim et al., 2005). However, no correlation between oxalic acid concentration and particle liquid water content was observed in aerosols collected from Mt. Hua in central China and the western North Pacific (Meng et al., 2014; Bikkina et al., 2015). In Mt. Hua, the oxalic acid concentration was observed to instead correlate with particle acidity. Acidic condition was suggested to be favorable for oxalic acid formation from isoprene and

monoterpene oxidation products in the aqueous-phase (Meng et al., 2014). Based on these results, it is therefore speculated that anthropogenic species like sulfate and nitrate that would influence the particle liquid water content and acidity in particles may affect the fate of intermediates from isoprene/monoterpenes/unsaturated fatty acids oxidation and thus the formation of DCA in SOA (Kawamura and Bikkina, 2016). Considering the wide distribution of DCA in the aerosols and their effects on climate, such kind of anthropogenic-biogenic interaction needs further exploration.

4. Effects of SO_2 on SOA formation from BVOCs photooxidation and ozonolysis

The anthropogenic sources of sulfur dioxide (SO_2) including fuel combustion, biomass burning, industrial activities comprise more than 78% of its global emission (Smith et al., 2001; Ye et al., 2018). SO_2 in the atmosphere not only acts as the primary source of acid precipitation and sulfate aerosol particles (Smith et al., 2001; Tao et al., 2013), but it also plays a great role in modifying SOA formation through sulfuric acid formation and corresponding acid-catalyzed heterogeneous reactions, reactions with reactive intermediates formed during VOCs oxidation, and perturbations on oxidation pathways (Jang et al., 2002; Boy et al., 2013; Friedman et al., 2016; Ye et al., 2018; Zhao et al., 2018b). The role of SO_2 (as well as sulfate discussed in section 2.2.2) in BVOCs oxidation is a typical anthropogenic-biogenic interaction influencing the biogenic SOA composition and budget (Kourtchev et al., 2014). A modeling work incorporating both SO_2 and sulfate (SOx) in eastern US saw a significant reduction of isoprene SOA as a result of a 25% SOx decrease (Pye et al., 2013). The removal of all anthropogenic SO_2 in the contiguous US was estimated to reduce the nationally averaged biogenic SOA by 14% (Carlton et al., 2018).

4.1 SO_2 effects on BVOCs photooxidation

The primary sink of SO_2 in the atmosphere is the reaction with ·OH, forming HSO_3 (R1) that can further react with O_2 to produce SO_3 and HO_2· (R2). The reaction between SO_3 and water vapor gives H_2SO_4 ultimately (R3).

$$\cdot OH + SO_2 + M \rightarrow HSO_3 + M \quad (R1)$$

$$HSO_3 + O_2 \rightarrow SO_3 + HO_2\cdot \quad (R2)$$

$$SO_3 + 2H_2O + M \rightarrow H_2SO_4 + H_2O + M \quad (R3)$$

Though numerous chamber experiments have shown enhanced SOA formation with particle acidity as described in section 3.2, the effect of SO_2 on SOA formation is not only limited to H_2SO_4 formation and corresponding acid-catalyzed reactions but also to its perturbation on the radical fate in the chamber. When the addition of SO_2 was disabled to change the radical level and thus gas-chemistry, the generation of H_2SO_4 increased linearly with initial SO_2 concentrations (Kleindienst et al., 2006). The enhanced SOA yield from isoprene and α-pinene photooxidation in the presence of SO_2 can be attributed to the acid-catalyzed reactions involving carbonyl compounds. Similarly, when excluding gas-phase chemistry during the photooxidation of limonene and α-pinene, the presence of SO_2 increased the SOA yield for these two hydrocarbons under both low and high NOx conditions (Zhao et al., 2018b). This was primarily because new particle formation induced by SO_2 oxidation could act as seeds to provide more surface and volume for the condensation of product vapors, though the effect of particle acidity may also exist. However, H_2SO_4-induced enhancement on SOA formation is not always the case for all VOC precursors. For example, in the photooxidation of cyclohexene under atmospheric relevant conditions, SO_2 was observed to suppress the SOA yield (Liu et al., 2017). Despite the oxidation of SO_2 by ·OH forms H_2SO_4 that can exert an enhancing effect on SOA formation, this effect is insufficient to compensate the simultaneously reduced ·OH reactivity towards

616 cyclohexene so that the net SO_2 effect is to weaken SOA formation. Another study
617 focusing on the effects of SO_2 on the α- and β-pinene photooxidation proposed that the
618 presence of SO_2 lead to enhanced products with a lesser degree of oxygenation but the
619 increased relative humidity dampened this enhancement (Friedman et al., 2016). Here,
620 the SO_2-induced change in the $\cdot OH/HO_2\cdot$ ratio and/or SO_3 reacting directly with
621 organic molecules were suggested to be responsible for the SO_2 perturbations. These
622 results indicate that, altogether, the perturbation of SO_2 on both particle- and gas-phase
623 reactions determine the extent to which SO_2 influences SOA formation. More BVOCs
624 photooxidation processes under atmospheric related conditions deserve continued focus.

625 ***4.2. SO_2 effects on BVOCs ozonolysis***

626 Besides reacting with ·OH, another important way for the transformation of SO_2 to
627 H_2SO_4 is by reacting with the stabilized Criegee Intermediates (sCIs) that are formed
628 during alkenes ozonolysis (Mauldin III et al., 2012; Boy et al., 2013; Sipila et al., 2014).
629 The reaction between SO_2 and sCIs forms SO_3, which further reacts efficiently with
630 water to produce H_2SO_4 as shown in Fig. 5. This none-·OH SO_2 oxidation pathway is
631 potentially responsible for the missing H_2SO_4 source in both boreal forest and coastal
632 sites (Mauldin III et al., 2012; Berresheim et al., 2014). Modeling results showed that
633 SO_2 oxidation by sCIs from monoterpenes ozonolysis accounted for about 60% of the
634 gas-phase SO_2 removal in tropical forest regions (Newland et al., 2018).

635 sCIs are key precursors to the formation of condensable species (Mackenzie-Rae
636 et al., 2018), such as carboxylic acid formed from sCIs isomerization, α-acyloxyalkyl
637 hydroperoxides formed from carboxylic acids + sCIs reactions and secondary ozonides
638 formed from carbonyl + sCIs reactions (Sipila et al., 2014; Chhantyal-Pun et al., 2018;
639 Zhao et al., 2019). SO_2 may influence SOA formation by altering sCIs chemistry and
640 H_2SO_4-related enhancement effects (Sipila et al., 2014). For example, it was found that

641 SOA formation from limonene ozonolysis was enhanced by the presence of SO_2,
642 regardless of dry (relative humidity (RH) < 16%) or humid (RH = ~ 50%) conditions
643 (Ye et al., 2018). Under dry conditions, the formation and condensation of H_2SO_4 from
644 the SO_2 + sCIs reaction and further acid-catalyzed reactions (Fig. 5) were expected for
645 the enhanced SOA yields. The composition analysis showed reduced oligomers but
646 enhanced organosulfates and oxidation state, suggesting that the H_2SO_4-related
647 enhancement overweighed the reduction of condensable species directly from sCIs
648 reactions. However, under humid conditions, the dominant SO_2 sink was proposed to
649 be its heterogeneous reaction with condensed-phase organic peroxides. A similar
650 pathway for the transformation of SO_2 to organosulfates was also characterized in the
651 case of α-pinene though SO_2 exhibited a minor effect on the SOA yield, likely because
652 the enhanced functionalization was offset by reduced oligomerization (Wang et al.,
653 2019). In addition, SO_2 also influences new particle formation during BVOCs
654 ozonolysis. In the absence of SO_2, new particle formation was not observed in the
655 ozonolysis of isoprene, α-pinene, β-pinene, and limonene under dry conditions.
656 However, with the addition of SO_2, new particle formation emerged and the amount of
657 nucleation was correlated with the sCIs yield (Stangl et al., 2019).

658 Water vapor is a potential competitor to SO_2 for sCIs to change the overall effect
659 of SO_2 on gas- and particle-phase reactions (Fig. 5), such as the masked SO_2 enhancing
660 effect on the SOA yield from butyl vinyl ether ozonolysis when RH > 40% (Huang et
661 al., 2015; Zhang et al., 2019a). This competition, however, highly depends on the
662 structure of the hydrocarbon itself (Vereecken et al., 2015). For monoterpene-derived
663 sCIs, their reactions with SO_2 are nearly independent of RH, implying minor
664 competitiveness of water than SO_2 even under high RH conditions (Sipila et al., 2014).
665 Nevertheless, observations for α-pinene and limonene ozonolysis still showed smaller

enhancement on particle volume concentration under humid condition (RH = ~ 50%) than under dry condition (RH = ~ 10%) (Ye et al., 2018). Besides the suppressed formation of high molecular weight species and organosulfates caused by water uptake and thus diluted particle acidity, a novel way for SO_2 to form organosulfates was proposed to be its heterogeneous reaction with organic (hydro-) peroxides (Fig. 5). It should be noted that this mechanism is still linked to uncertainties and needs continued focus. Besides, the effects of SO_2 on SOA formation from the ozonolysis of other BVOCs such as isoprene and sesquiterpenes are still scarcely studied and warrant more attention to better evaluate SO_2-involved anthropogenic-biogenic interactions at night.

5. Effects of NH_3 and amines on SOA formation and aging

NH_3 and amines, both of which play a key role in acid rain, nitrogen deposition, and fine particle pollution, are ubiquitous in the atmosphere (Liu et al., 2019). The anthropogenic sources of NH_3 and amines include fertilizer use, animal husbandry, industries, sewage treatment, and automobiles (Ge et al., 2011; Zeng et al., 2018). With these emission sources, a substantial increase of NH_3 emission has been seen over the European Union (1.83% yr^{-1}), China (2.27% yr^{-1}), and the US (2.61% yr^{-1}) from the year 2002 to 2016 (Warner et al., 2017). The typical concentration of atmospheric amines is estimated to be about 1-2 orders of magnitude lower than that of NH_3 (Ge et al., 2011; Qiu and Zhang, 2013). In addition to directly contributing to fine particulate matter by reacting with sulfuric or nitric acid to generate secondary inorganic aerosols (ammonium sulfate, ammonium bisulfate and ammonium nitrate), NH_3 and amines can also influence SOA yields and composition through both gas-phase and heterogeneous reactions (Zhu et al., 2013; Babar et al., 2017; Niu et al., 2017).

5.1 NH_3 effects on SOA formation

The potential role of NH_3 in SOA formation was first investigated in the styrene ozonolysis system (Na et al., 2006). The addition of excessive NH_3 into the chamber where SOA formation had ceased resulted in the decreased aerosol volume concentration, which was attributed to the rapid decomposition of the main SOA-forming species (3,5-diphenyl-1,2,4-trioxolane and the hydroxyl-substituted ester) caused by the nucleophilic attack of NH_3. When styrene ozonolysis was further studied in the presence of NH_3, the SOA yield was significantly reduced (Ma et al., 2018). Quantum chemical calculations revealed that the reaction between NH_3 and sCIs suppressed the formation of condensable secondary ozonide (3,5-diphenyl-1,2,4-trioxolane) that was formed via sCIs + aldehyde reaction. Different from styrene, NH_3 exhibited an enhancement effect on the particle growth and SOA yield from α-pinene ozonolysis whether NH_3 was added in the beginning or at the end of the reaction (Na et al., 2007; Babar et al., 2017). Ammonium salts generated via the gas-phase reaction between NH_3 and organic acids (such as pinic acid, pinonic acid) nucleated and contributed to the increased SOA formation. In the photooxidation of α-pinene in the presence of NH_3, particle-phase ammonium correlated well with organic mono- and di-carboxylic acids in the gas-phase, highlighting the central role of ammonium salts formed via acid-base reaction between NH_3 and organic acids in SOA formation (Hao et al., 2020). Similarly, the ozonolysis of limonene and BVOCs mixture (emitted from cleaning products) in the presence of NH_3 yielded 60% and 35% higher maximum total particle number concentrations than those in the absence of NH_3 (Huang et al., 2012; Niu et al., 2017). Both nuclei coagulation and condensation caused by acid-base reaction were responsible for the SOA growth. But for SOA from isoprene ozonolysis, its reaction with NH_3 did not significantly change particle number and volume concentrations, suggesting that not all gas-phase organic acids (e.g., 2-methylglyceric

acid, pyruvic acid) could experience gas-to-particle conversion through acid-base reaction (Na et al., 2007).

5.2 NH_3 effects on SOA aging

Heterogeneous uptake of NH_3 by SOA is an important way to complex SOA composition and optical properties by forming N-containing organic compounds (NOC). NOC are regarded as a significant class of heteroatom-containing brown carbon (BrC) compounds that absorb light with a strong wavelength dependence (Liu et al. (2015) and reference therein). SOA from limonene ozonolysis was the first biogenic SOA that had been found to turn to be more light-absorbing when aqueous extract of SOA was aged by ammonium ions (Bones et al., 2010). The key aging reactions involve firstly the acid-catalyzed transformation of carbonyls to primary imines (Fig. 6 (a)). Particularly, imines formed via the reaction between NH_4^+ and 1,5-dicarbonyl compounds from limonene SOA may undergo cyclization to give the dihydropyridinium ion (Fig. 6 (b)). The combination product of two dihydropyridinium ions further disproportionates, finally leading to conjugated NOC that are responsible for the enhanced light absorption. A similar NH_3 effect on the light absorption of SOA has been further observed when exposing NH_3 directly to SOA from the photooxidation or ozonolysis of various biogenic as well as anthropogenic VOCs (Laskin et al., 2010; Updyke et al., 2012; Lee et al., 2013; Babar et al., 2017). The light absorption of aged SOA from ozonolysis was generally stronger than that from ·OH oxidation, confirming the role of the carbonyl + NH_3 reaction in NOC formation as alkene ozonolysis yields more carbonyl than ·OH-initiated oxidation (Updyke et al., 2012). Besides the heterocyclic NOC formation through the intramolecular cyclization of the primary imine, the reaction between primary imines with another carbonyl that leads to a more stable secondary imine (Schiff base formation) (Fig. 6 (c)) and the 1,2-dicarbonyls +

740 aldehydes reaction in the presence of NH_3 that gives imidazoles (Fig. 6 (d)) are likely
741 to induce light-absorbing products in aged SOA (Laskin et al., 2010; Updyke et al.,
742 2012; Laskin et al., 2014). Very recently, uptake coefficients of NH_3 onto SOA from
743 α-pinene ozonolysis or *m*-xylene ·OH-oxidation were observed to be positively
744 correlated with the acidity of aerosol and negatively correlated with the concentration
745 of NH_3, kinetically confirming that NOCs were formed via heterogeneous reaction of
746 NH_3 with SOA (Liu et al., 2015). It should be noted that some BrC formed via the
747 mechanism discussed above may be unstable towards sunlight or oxidants but need
748 further exploration (Sareen et al., 2013; Lee et al., 2014). Regardless, considering the
749 increase trend of NH_3 emission, NH_3 is of great significance to mediate the components
750 and physical properties of biogenic SOA. Hence, more relevant studies are warranted.

751 ***5.3 Amine-involved particle-phase reactions***

752 As derivatives of ammonia, amines have been observed in both gas- and particle-
753 phases (Ge et al., 2011). Though they can participate in SOA formation via various
754 pathways, here we only focus on those likely occurring during biogenic SOA formation.
755 Amine-epoxide reactions were proposed to be kinetically feasible for isoprene-derived
756 epoxides and high amine SOA concentrations (Stropoli and Elrod, 2015). However, it
757 should be noted that such reactions can only be favored when the pH values of the
758 reaction environment are higher than the pKa values of particular amines. The prevalent
759 acidic SOA in the atmosphere may not be conducive to such reactions.

760 Similar to NH_3, amines could also engage in the heterogeneous reactions with
761 carbonyls to form imine/enamine compounds (Zhang et al., 2015). The particle-phase
762 reaction between methylamine and glyoxal that is mainly derived from biogenic sources
763 showed that glyoxal could irreversibly trap amines in the aerosol-phase and convert
764 them into oligomers (De Haan et al., 2009). SOA formed through this pathway were

765 estimated to be up to 11 Tg yr^{-1} globally if glyoxal was consumed exclusively in this
766 path. To explain the formation of high molecular weight NOC observed in ambient
767 aerosols, the Mannich reaction among amines (or ammonia), aldehydes, and carbonyls
768 with an adjacent, acidic proton was proposed (Wang et al., 2010).

769 Acid-base reactions are another class of amine-involved reactions of interest. The
770 heterogeneous uptake of methylamine, dimethylamine, and trimethylamine onto citric
771 acid and humic acid confirmed acid-base reactions between amines and carboxylic
772 acids (Liu et al., 2012). Aminium salts formed would enhance the water uptake of
773 particles and thus alter the particle properties. Based on the equilibrium partitioning of
774 dimethylamine, ammonia, acetic acid, pinic acid and their salts, amines were suggested
775 to contribute significantly to the formation of organic salts that might have a potential
776 contribution to new particle growth (Barsanti et al., 2009). Theoretical calculations for
777 the thermodynamics of accretion reactions between organic acids (malic, maleic, and
778 pinic acids) and amines showed that such interactions could contribute to SOA
779 formation via the kinetically favored formation of ester and amide (Barsanti and
780 Pankow, 2006). Additionally, new particle formation in a flow tube was also
781 considerably enhanced when amines reacted with methanesulfonic acid in the presence
782 of water (Dawson et al., 2012). Considering that epoxides, carbonyls and organic acids
783 are important BVOCs oxidation products, it is plausible that the reactions between
784 amines and epoxides/carbonyls/acids from BVOCs oxidation may influence biogenic
785 SOA formation but current studies on this process are still limited and thus need
786 furthermore attention.

787 **6. Anthropogenic-biogenic interactions in China**

788 Many areas in China have been suffering severe haze events in the last few years
789 (Li et al., 2017a; Zhao et al., 2018a; Lu et al., 2019). Though great efforts have been

790 devoted to mitigating haze pollution by controlling various anthropogenic emissions
791 (Xia et al., 2016), high mixing ratios of SO_2, NOx and NH_3 can still be observed to
792 exceed 100 ppb and the contribution of POA to total submicron aerosol is up to 27% in
793 regions like North China Plain (Li et al., 2017a; Meng et al., 2018). While SOA derived
794 from anthropogenic precursors, such as those VOCs emitted from traffic/coal burning
795 account for a significant fraction of fine particles, biogenic SOA also has a contribution
796 and shows seasonal and regional dependence (Ding et al., 2014; Huang et al., 2014;
797 Zhang et al., 2017b; Xing et al., 2019). Biogenic emissions in China were estimated to
798 be 23.54 Tg yr^{-1} and contributed approximately for 70% of the total SOA in summer
799 (Wu et al., 2020). Considering that anthropogenic emissions and BVOCs may coexist
800 abundantly in regions like Pearl River Delta, Yangtze River Delta, Sichuan Basin, and
801 North China Plain, there are some evidences showing that anthropogenic-biogenic
802 interactions are important in SOA formation in these regions, as Fig. 7 and Table 3
803 summarized (He et al., 2014; Hu et al., 2017; He et al., 2018; Zhang et al., 2019b; Wu
804 et al., 2020).

805 Biogenic organosulfates in ambient particles, which are formed through the cross-
806 reaction between BVOCs and anthropogenic pollutants, are important markers of
807 anthropogenic-biogenic interactions. Quantification of organosulfates in fine particle
808 samples collected in the central Pearl River Delta in 2010 showed nearly three times
809 higher pinene-derived nitrooxyorganosulfates (MW = 295) in fall than in summer,
810 probably due to the higher levels of sulfates and NOx in fall (He et al., 2014). 2-
811 Methyltetrol sulfate ester produced via isoprene-derived IEPOX oxidation under low
812 NOx condition showed low concentration. The high NOx mixing ratio (daily 65 ppb
813 and hourly 163 ppb) here could be the reason why IEPOX formation was suppressed.
814 Other observations in this region also showed the Ox and sulfate dependence of

isoprene-SOA tracers (He et al., 2018; Zhang et al., 2019b). Simultaneously, SOA tracers originating from *β*-caryophyllene and high-generation monoterpene oxidation were positively correlated with Ox and sulfate (Zhang et al., 2019b). Interestingly, the reduction of 50% Ox in this region was estimated to be more efficient in reducing biogenic SOA than that of sulfate. In eastern China, combining field measurements and model analysis, the depression of IEPOX SOA by high NOx level was confirmed as the reactive uptake of IEPOX and the ratio of IEPOX to isoprene high-NOx SOA precursors were lower than those observed in regions with abundant biogenic emissions, high particle acidity and low NOx concentration (Zhang et al., 2017c). Biogenic SOA formation in summer 2012 over China was simulated using the Community Multiscale Air Quality (CMAQ) model that considers reactive uptake of isoprene-derived intermediates, multigenerational oxidation and detailed monoterpene SOA production (Qin et al., 2018a). Isoprene SOA tracers showed high concentrations in southwestern China due to the abundant IEPOX and high particle surface area provided by sulfate. Similar positive correlations between biogenic SOA tracers and sulfate were also observed in urban Urumqi, Qinghai Lake and urban Xi'an, Beijing, Nanjing, Pearl River Delta, and Wangqingshan (He et al., 2014; Zhang et al., 2017c; He et al., 2018; Ren et al., 2018; Zhang et al., 2019b; Bryant et al., 2020). Isoprene SOA formation pathway in some areas of the Yangtze River Delta Region and North China Plain was influenced by NOx emission, as a high ratio of 2-methylglyceric acid and 2-methyltetrols (0.06-0.1 by model and 0.58-0.78 by observation) showed in these regions (Qin et al., 2018a). We note that though the simulated total biogenic SOA in summer 2012 in China accurately tracked the observed data (normalized mean bias of 1% and r^2 of 0.59), CMAQ did not well simulate the ratios of 2-methylglyceric acid and 2-methyltetrols. The uncertainties in the fate of IEPOX, 2-methylglyceric acid

reaction parameters and C5-alkene triols formation pathways could be possible reasons for the discrepancies between modeled and observed results. The linear correlations between SOA tracers of isoprene, monoterpenes and sesquiterpenes and anthropogenic pollutants, such as SO_2 and NOx were also observed at Mountain Wuyi and Changbai in southeastern and northeastern China, respectively, suggesting that SO_2 and NOx can enhance biogenic SOA production in the remote mountain area through acid-catalyzed heterogeneous chemistry (Wang et al., 2008; Ren et al., 2019). For more polluted urban Beijing that is characterized by both local isoprene and anthropogenic pollutants, anthropogenic-influenced biogenic SOA formation in summer 2017 was also observed (Bryant et al., 2020). Isoprene-derived particulate organosulfates and nitrooxy-organosulfates, the formation of which is related to NOx and particulate SO_4^{2-} level, accounted for 0.62% and could be as high as ~ 3% on certain days.

For China as a whole, SOA formation in 2013 was modeled by incorporating updated two-product SOA yields and SOA formation from reactive uptake of isoprene-derived IEPOX and methacrylic acid epoxide into the updated 3-D air quality model (Hu et al., 2017). The enhancement effect of anthropogenic emission on biogenic SOA was evidenced because the SOA concentration was less than 1 μg m^{-3} when solely considering biogenic emissions (Hu et al., 2017). Similar anthropogenic-biogenic interactions were found in a more recent study (Wu et al., 2020). With the modeled anthropogenic and biogenic emission in China in 2016, the CMAQ model that includes updated POA aging, SOA properties and IEPOX organosulfates formation rate constants showed that removing all anthropogenic emissions while keeping biogenic emissions unchanged lead to a 60% reduction of SOA formation. These studies suggest that though the emission of BVOCs is uncontrollable, biogenic SOA reduction can be achieved through controlling anthropogenic emissions. It should be noted that the

modeled SOA concentrations have not been compared with the direct SOA measurements due to data limitations. Many other studies show that current models usually underestimate or predict the SOA concentration with large uncertainties due to the missed SOA precursors, formation mechanism, components and complex atmospheric conditions (Shrivastava et al., 2017; Liu et al., 2018; Slade et al., 2019). With more detailed measurements of the particle composition and biogenic SOA tracer performed in many areas over China (Table 3) and the increased knowledge of SOA formation mechanism by laboratory studies, models could be better constrained by the observed data and models' performance could be better evaluated.

7. Summary and outlook

Accurate predictions of air pollution, climate change and health effects of SOA requires a more accurate assessment of the regional and global SOA budget. Reducing the SOA burden uncertainty between modeling and observation needs better speciation and quantification of SOA precursors and formation pathways under atmospheric-relevant conditions. As one uncontrollable and largest SOA source, BVOCs contribute significantly to the regional and global SOA formation but the extent of this contribution is mediated by anthropogenic emissions.

Currently available laboratory and field observations have made great progress in the scientific understanding of this kind of interaction. This paper reviews the effects of NOx, anthropogenic aerosols, SO_2 and NH_3/amines on biogenic SOA formation from BVOCs photooxidation and ozonolysis, from the perspective of gas- and particle-phase reactions. NOx level is effective in determining the $RO_2\cdot$ fate by competing with $HO_2\cdot$ in daytime oxidation and changing atmospheric oxidation capacity by forming $NO_3\cdot$ that acts as another sink for BVOCs besides O_3 at night. These NOx-involved BVOCs oxidation processes induce changes in the distribution of product volatility and

thus SOA composition and yields. But whether high NOx or low NOx levels favors SOA formation depends on the hydrocarbon precursor itself, indicating that the spatial and temporal distribution of different BVOCs need to be carefully considered when evaluating NOx effects on biogenic SOA formation. The definition of high NOx or low NOx level for a specific BVOC, such as isoprene is also unclear and a detailed NOx-involved mechanism warrants further attention.

POA from anthropogenic activity could alter the gas-particle partition of SOA-forming products if a homogeneous mixing phase occurs. Inorganic sulfates promote SOA formation through particle-phase reactions, which would simultaneously be associated with the particle acidity and water content. While the strong correlation between IEPOX SOA and sulfates is frequently observed, the combined effects of these factors under certain circumstances should be checked in detail by further laboratory experiments.

SO_2 enhances SOA formation dominantly by forming H_2SO_4 that triggers new particle formation and acid-catalyzed particle-phase reactions. SO_2-introduced reduction of the oxidation capacity, such as ·OH and sCIs levels in the reaction system would somewhat counterbalance the enhancement effect. New mechanism of the direct interaction between SO_2 and peroxides and other potential mechanism are possible but need further examination.

The acid-base reaction between NH_3 and organic acid in the gas-phase is the main way for the interference of NH_3 on SOA generation. Whether NH_3 enhances particle formation depends on organic acids formed from BVOCs oxidation and thus the parent BVOCs and oxidants themselves. The particle-phase reaction between ammonia and carbonyls under acid condition is efficient in forming NOC and thus enhancing the light absorption of SOA particles. The reactions of amines with epoxides/carbonyls/organic

acids that derived from biogenic sources also possibly modify biogenic SOA composition and properties but need further exploration.

Despite the abovementioned advances have shed light on the importance of anthropogenic-biogenic interactions, the exploration of this topic is far from complete. More research efforts are recommended to be engaged toward the following directions.

(1) Generally, the concentrations of parent hydrocarbons and anthropogenic pollutants in laboratory experiments are much higher than the ambient levels, which might cause a deviation in some critical conditions, such as the change of the competitive advantages of different reaction paths. Therefore, the concentrations of the substance in the laboratory experiments need to be closer to the real atmospheric level while keeping other conditions, like RH, particle acidity more atmospheric-relevant.

(2) Besides the role of single pollutant in the formation of biogenic SOA, the combined effects of multiple anthropogenic pollutants, such as the simultaneous presence of NOx and SO_2, SO_2 and NH_3/amines in BVOCs photooxidation and ozonolysis are scarcely investigated. Giving chemical insights into whether obvious synergistic, antagonistic actions, or irrelevance between different pollutants exist makes sense because these interactions could largely affect the SOA yield.

(3) SOA tracers, such as organosulfates, organic nitrates from typical BVOCs are important compounds found in laboratory and field SOA samples. These compounds not only qualitatively represent anthropogenic biogenic-interactions, but their atmospheric concentrations could also be the basis for the quantification of controllable biogenic SOA. While using surrogate compounds for the quantification of these SOA tracers induces uncertainty, authentic quantitative standards can further assist in the accurate quantification and comprehensive interpretation of the mechanism for the interaction between BVOCs and human-made pollutants. These authentic quantitative

standards that can be used for the determination of SOA from various monoterpenes and sesquiterpenes are yet often unavailable and require further development.

(4) The particle phase state (liquid, semisolid, solid) of SOA is crucial for the partitioning of semi-volatile compounds, particle-phase reactions and, most importantly, climate. SOA morphology is related to the components and their hygroscopicity, for example, the presence of oligomers and high molecular weight compounds favors the amorphous solid state of SOA particles while hydrophilic products lead to a liquid state of the particles. Anthropogenic pollutants, such as NOx, SO_2 and particle acidity could potentially change biogenic SOA formation pathways and composition, and thus possibly the phase state of SOA particles. However, this is still poorly understood. Future research needs to expand on the exploration of anthropogenic effects on the morphology of SOA to better address the morphology-associated heterogeneous chemistry, optical properties, air quality and climate.

(5) Vast areas of the globe, like China, still experience both large BVOCs and anthropogenic pollutant emissions. To explore the extent to which biogenic SOA could be mitigated by controlling anthropogenic pollutants, collecting more field evidence regarding the correlation between regional-specific types and amount of BVOCs and human-induced pollutants is a demanding task. Furthermore, while the climate change and land use change tend to increase the global BVOC emissions, emissions of anthropogenic pollutants are also changing. For example, NOx and SO_2 emissions are expected to continually decrease in North America and Europe but to increase in Asia. Besides the interaction mechanism among different BVOCs precursors and pollutants, changes in the temporal and spatial distribution of both BVOCs and anthropogenic pollutants should be the basis for the regional and, ultimately, global control of SOA formation.

Overall, shedding light on the anthropogenic-biogenic interactions is necessary for the better evaluation of the contribution of biogenic SOA to the total SOA budget, formulating more effective pollution control measures and reducing uncertainties in the current understanding of air pollution and climate change.

Acknowledgements. This work was supported by National Natural Science Foundation of China (91644214), Youth Innovation Program of Universities in Shandong Province (2019KJD007), and Fundamental Research Fund of Shandong University (2020QNQT012).

REFERENCES

Alfarra, M. R., and Coauthors, 2012: The effect of photochemical ageing and initial precursor concentration on the composition and hygroscopic properties of β-caryophyllene secondary organic aerosol. *Atmos. Chem. Phys.*, **12**, 6417-6436.

Asa-Awuku, A., M. A. Miracolo, J. H. Kroll, A. L. Robinson, and N. M. Donahue, 2009: Mixing and phase partitioning of primary and secondary organic aerosols. *Geophys. Res. Lett.*, **36**, L15827.

Atkinson, R., 2000: Atmospheric chemistry of VOCs and NOx. *Atmos. Environ.*, **34**, 2063-2101.

Atkinson, R., and J. Arey, 1998: Atmospheric chemistry of biogenic organic compounds. *Accounts Chem. Res.*, **31**, 574-583.

Ayres, B. R., and Coauthors, 2015: Organic nitrate aerosol formation via NO_3 + biogenic volatile organic compounds in the southeastern United States. *Atmos. Chem. Phys.*, **15**, 13377-13392.

Babar, Z. B., J.-H. Park, and H.-J. Lim, 2017: Influence of NH_3 on secondary organic aerosols from the ozonolysis and photooxidation of α-pinene in a flow reactor. *Atmos. Environ.*, **164**, 71-84.

Berresheim, H., and Coauthors, 2014: Missing SO_2 oxidant in the coastal atmosphere? – observations from high-resolution measurements of OH and atmospheric sulfur compounds. *Atmos. Chem. Phys.*, **14**, 12209-12223.

Bikkina, S., K. Kawamura, and Y. Miyazaki, 2015: Latitudinal distributions of atmospheric dicarboxylic acids, oxocarboxylic acids, and α-dicarbonyls over the western North Pacific: Sources and formation pathways. *J. Geophys. Res. Atmos.*, **120**, 5010-5035.

Bikkina, S., K. Kawamura, Y. Miyazaki, and P. Fu, 2014: High abundances of oxalic,

azelaic, and glyoxylic acids and methylglyoxal in the open ocean with high biological activity: Implication for secondary OA formation from isoprene. *Geophys. Res. Lett.*, **41**, 3649-3657.

Bones, D. L., and Coauthors, 2010: Appearance of strong absorbers and fluorophores in limonene-O_3 secondary organic aerosol due to NH_4^+-mediated chemical aging over long time scales. *J. Geophys. Res.*, **115**, D05203.

Boy, M., and Coauthors, 2013: Oxidation of SO_2 by stabilized Criegee intermediate (sCI) radicals as a crucial source for atmospheric sulfuric acid concentrations. *Atmos. Chem. Phys.*, **13**, 3865-3879.

Brown, S. S., and J. Stutz, 2012: Nighttime radical observations and chemistry. *Chem. Soc. Rev.*, **41**, 6405-6447.

Brown, S. S., and Coauthors, 2013: Biogenic VOC oxidation and organic aerosol formation in an urban nocturnal boundary layer: Aircraft vertical profiles in Houston, TX. *Atmos. Chem. Phys.*, **13**, 11317-11337.

Bryant, D. J., and Coauthors, 2020: Strong anthropogenic control of secondary organic aerosol formation from isoprene in Beijing. *Atmos. Chem. Phys.*, **20**, 7531–7552.

Budisulistiorini, S. H., and Coauthors, 2013: Real-time continuous characterization of secondary organic aerosol derived from isoprene epoxydiols in downtown Atlanta, Georgia, using the Aerodyne Aerosol Chemical Speciation Monitor. *Environ. Sci. Technol.*, **47**, 5686-5694.

Budisulistiorini, S. H., and Coauthors, 2015: Examining the effects of anthropogenic emissions on isoprene-derived secondary organic aerosol formation during the 2013 Southern Oxidant and Aerosol Study (SOAS) at the Look Rock, Tennessee ground site. *Atmos. Chem. Phys.*, **15**, 8871-8888.

Cappa, C. D., S. H. Jathar, M. J. Kleeman, K. S. Docherty, J. L. Jimenez, J. H. Seinfeld,

and A. S. Wexler, 2016: Simulating secondary organic aerosol in a regional air quality model using the statistical oxidation model – Part 2: Assessing the influence of vapor wall losses. *Atmos. Chem. Phys.*, **16**, 3041-3059.

Carlton, A. G., R. W. Pinder, P. V. Bhave, and G. A. Pouliot, 2010: To what extent can biogenic SOA be controlled? *Environ. Sci. Technol.*, **44**, 3376-3380.

Carlton, A. G., H. O. T. Pye, K. R. Baker, and C. J. Hennigan, 2018: Additional benefits of federal air-quality rules: model estimates of controllable biogenic secondary organic aerosol. *Environ. Sci. Technol.*, **52**, 9254-9265.

Carlton, A. G., B. J. Turpin, K. E. Altieri, S. Seitzinger, A. Reff, H.-J. Lim, and B. Ervens, 2007: Atmospheric oxalic acid and SOA production from glyoxal: Results of aqueous photooxidation experiments. *Atmos. Environ.*, **41**, 7588-7602.

Carslaw, K. S., and Coauthors, 2013: Large contribution of natural aerosols to uncertainty in indirect forcing. *Nature*, **503**, 67-71.

Chan, A. W. H., and Coauthors, 2010: Role of aldehyde chemistry and NOx concentrations in secondary organic aerosol formation. *Atmos. Chem. Phys.*, **10**, 7169-7188.

Chen, F., H. Zhou, J. Gao, and P. K. Hopke, 2017: A chamber study of secondary organic Aerosol (SOA) formed by ozonolysis of d-Limonene in the presence of NO. *Aerosol Air Qual. Res.*, **17**, 59-68.

Chhantyal-Pun, R., and Coauthors, 2018: Criegee Intermediate Reactions with Carboxylic Acids: A Potential Source of Secondary Organic Aerosol in the Atmosphere. *ACS Earth Space Chem.*, **2**, 833-842.

Chi, X., and Coauthors, 2018: Acidity of aerosols during winter heavy haze events in Beijing and Gucheng, China. *J. Meteorol. Res.*, **32**, 14-25.

Couvidat, F., M. G. Vivanco, and B. Bessagnet, 2018: Simulating secondary organic

aerosol from anthropogenic and biogenic precursors: Comparison to outdoor chamber experiments, effect of oligomerization on SOA formation and reactive uptake of aldehydes. *Atmos. Chem. Phys.*, **18**, 15743-15766.

Czoschke, N. M., M. Jang, and R. M. Kamens, 2003: Effect of acidic seed on biogenic secondary organic aerosol growth. *Atmos. Environ.*, **37**, 4287-4299.

Darer, A. I., N. C. Cole-Filipiak, A. E. O'Connor, and M. J. Elrod, 2011: Formation and stability of atmospherically relevant isoprene-derived organosulfates and organonitrates. *Environ. Sci. Technol.*, **45**, 1895-1902.

Ding, X., Q.-F. He, R.-Q. Shen, Q.-Q. Yu, and X.-M. Wang, 2014: Spatial distributions of secondary organic aerosols from isoprene, monoterpenes, β-caryophyllene, and aromatics over China during summer. *J. Geophys. Res. Atmos.*, **119**, 11877-11891.

Dommen, J., and Coauthors, 2006: Laboratory observation of oligomers in the aerosol from isoprene/NOx photooxidation. *Geophys. Res. Lett.*, **33**, L13805.

Donahue, N. M., A. L. Robinson, C. O. Stanier, and S. N. Pandis, 2006: Coupled partitioning, dilution, and chemical aging of semivolatile organics. *Environ. Sci. Technol.*, **40**, 2635-2643.

Draper, D. C., D. K. Farmer, Y. Desyaterik, and J. L. Fry, 2015: A qualitative comparison of secondary organic aerosol yields and composition from ozonolysis of monoterpenes at varying concentrations of NO_2. *Atmos. Chem. Phys.*, **15**, 12267-12281.

Eddingsaas, N. C., and Coauthors, 2012: α-Pinene photooxidation under controlled chemical conditions - Part 2: SOA yield and composition in low- and high-NOx environments. *Atmos. Chem. Phys.*, **12**, 7413-7427.

Edwards, P. M., and Coauthors, 2017: Transition from high- to low-NOx control of night-time oxidation in the southeastern US. *Nat. Geosci.*, **10**, 490-495.

Ehn, M., and Coauthors, 2014: A large source of low-volatility secondary organic

aerosol. *Nature*, **506**, 476-479.

Emanuelsson, E. U., and Coauthors, 2013: Formation of anthropogenic secondary organic aerosol (SOA) and its influence on biogenic SOA properties. *Atmos. Chem. Phys.*, **13**, 2837-2855.

Ensberg, J. J., and Coauthors, 2014: Emission factor ratios, SOA mass yields, and the impact of vehicular emissions on SOA formation. *Atmos. Chem. Phys.*, **14**, 2383-2397.

Ervens, B., B. J. Turpin, and R. J. Weber, 2011: Secondary organic aerosol formation in cloud droplets and aqueous particles (aqSOA): A review of laboratory, field and model studies. *Atmos. Chem. Phys.*, **11**, 11069-11102.

Farina, S. C., P. J. Adams, and S. N. Pandis, 2010: Modeling global secondary organic aerosol formation and processing with the volatility basis set: Implications for anthropogenic secondary organic aerosol. *J. Geophys. Res. Atmos.*, **115**, D09202.

Faust, J. A., J. P. Wong, A. K. Lee, and J. P. Abbatt, 2017: Role of aerosol liquid water in secondary organic aerosol formation from volatile organic compounds. *Environ. Sci. Technol.*, **51**, 1405-1413.

Fouqueau, A., M. Cirtog, M. Cazaunau, E. Pangui, J.-F. Doussin, and B. Picquet-Varrault, 2020: A comparative and experimental study of the reactivity with nitrate radical of two terpenes: α-terpinene and γ-terpinene. *Atmos. Chem. Phys. Discuss.*, https://doi.org/10.5194/acp-2020-5504.

Friedman, B., P. Brophy, W. H. Brune, and D. K. Farmer, 2016: Anthropogenic sulfur perturbations on biogenic oxidation: SO_2 additions impact gas-phase OH oxidation products of α- and β-Pinene. *Environ. Sci. Technol.*, **50**, 1269-1279.

Fry, J. L., and Coauthors, 2014: Secondary organic aerosol formation and organic nitrate yield from NO_3 oxidation of biogenic hydrocarbons. *Environ. Sci. Technol.*, **48**, 11944-11953.

Fry, J. L., and Coauthors, 2009: Organic nitrate and secondary organic aerosol yield from NO_3 oxidation of β-pinene evaluated using a gas-phase kinetics/aerosol partitioning model. *Atmos. Chem. Phys.*, **9**, 1431-1449.

Fry, J. L., and Coauthors, 2013: Observations of gas- and aerosol-phase organic nitrates at BEACHON-RoMBAS 2011. *Atmos. Chem. Phys.*, **13**, 8585-8605.

Fry, J. L., and Coauthors, 2018: Secondary organic aerosol (SOA) yields from NO_3 + isoprene based on nighttime aircraft power plant plume transects. *Atmos. Chem. Phys.*, **18**, 11663-11682.

Fu, T.-M., D. J. Jacob, F. Wittrock, J. P. Burrows, M. Vrekoussis, and D. K. Henze, 2008: Global budgets of atmospheric glyoxal and methylglyoxal, and implications for formation of secondary organic aerosols. *J. Geophys. Res.*, **113**, D15303.

Gao, S., and Coauthors, 2004: Particle phase acidity and oligomer formation in secondary organic aerosol. *Environ. Sci. Technol.*, **38**, 6582-6589.

Gaston, C. J., T. P. Riedel, Z. Zhang, A. Gold, J. D. Surratt, and J. A. Thornton, 2014: Reactive uptake of an isoprene-derived epoxydiol to submicron aerosol particles. *Environ. Sci. Technol.*, **48**, 11178-11186.

Ge, X., A. S. Wexler, and S. L. Clegg, 2011: Atmospheric amines – Part I. A review. *Atmos. Environ.*, **45**, 524-546.

George, C., M. Ammann, B. D'Anna, D. J. Donaldson, and S. A. Nizkorodov, 2015: Heterogeneous photochemistry in the atmosphere. *Chem. Rev.*, **115**, 4218-4258.

Glasius, M., and A. H. Goldstein, 2016: Recent discoveries and future challenges in atmospheric organic chemistry. *Environ. Sci. Technol.*, **50**, 2754-2764.

Goldstein, A. H., C. D. Koven, C. L. Heald, and I. Y. Fung, 2009: Biogenic carbon and anthropogenic pollutants combine to form a cooling haze over the southeastern United States. *Proc. Natl. Acad. Sci. U.S.A.*, **106**, 8835-8840.

Griffin, R. J., D. R. Cocker, R. C. Flagan, and J. H. Seinfeld, 1999: Organic aerosol formation from the oxidation of biogenic hydrocarbons. *J. Geophys. Res. Atmos.*, **104**, 3555-3567.

Guenther, A. B., X. Jiang, C. L. Heald, T. Sakulyanontvittaya, T. Duhl, L. K. Emmons, and X. Wang, 2012: The Model of Emissions of Gases and Aerosols from Nature version 2.1 (MEGAN2.1): An extended and updated framework for modeling biogenic emissions. *Geosci. Model Dev.*, **5**, 1471-1492.

Guo, H., and Coauthors, 2015: Fine-particle water and pH in the southeastern United States. *Atmos. Chem. Phys.*, **15**, 5211-5228.

Hallquist, M., I. Wangberg, E. Ljungstrom, I. Barnes, and K. H. Becker, 1999: Aerosol and product yields from NO_3 radical-initiated oxidation of selected monoterpenes. *Environ. Sci. Technol.*, **33**, 553-559.

Hallquist, M., and Coauthors, 2009: The formation, properties and impact of secondary organic aerosol: current and emerging issues. *Atmos. Chem. Phys.*, **9**, 5155-5236.

Han, Y., C. A. Stroud, J. Liggio, and S.-M. Li, 2016: The effect of particle acidity on secondary organic aerosol formation from α-pinene photooxidation under atmospherically relevant conditions. *Atmos. Chem. Phys.*, **16**, 13929-13944.

Hao, L., E. Kari, A. Leskinen, D. R. Worsnop, and A. Virtanen, 2020: Direct contribution of ammonia to CCN-size α-pinene secondary organic aerosol formation. *Atmos. Chem. Phys. Discuss.*, https://doi.org/10.5194/acp-2020-5457.

Hayes, P. L., and Coauthors, 2015: Modeling the formation and aging of secondary organic aerosols in Los Angeles during CalNex 2010. *Atmos. Chem. Phys.*, **15**, 5773-5801.

He, Q. F., and Coauthors, 2018: Secondary organic aerosol formation from isoprene epoxides in the Pearl River Delta, south China: IEPOX- and HMML-derived tracers. *J.*

Geophys. Res. Atmos., **123**, 6999-7012.

He, Q. F., and Coauthors, 2014: Organosulfates from pinene and isoprene over the Pearl River Delta, South China: seasonal variation and implication in formation mechanisms. *Environ. Sci. Technol.*, **48**, 9236-9245.

Heald, C. L., and Coauthors, 2008: Predicted change in global secondary organic aerosol concentrations in response to future climate, emissions, and land use change. *J. Geophys. Res. Atmos.*, **113**, D05211.

Hennigan, C. J., J. Izumi, A. P. Sullivan, R. J. Weber, and A. Nenes, 2015: A critical evaluation of proxy methods used to estimate the acidity of atmospheric particles. *Atmos. Chem. Phys.*, **15**, 2775-2790.

Hessberg, C. v., P. v. Hessberg, U. Pöschl, M. Bilde, O. J. Nielsen, and G. Moortgat, 2009: Temperature and humidity dependence of secondary organic aerosol yield from the ozonolysis of β-pinene. *Atmos. Chem. Phys.*, **9**, 3583-3599.

Hettiyadura, A. P. S., I. M. Al-Naiema, D. D. Hughes, T. Fang, and E. A. Stone, 2019: Organosulfates in Atlanta, Georgia: Anthropogenic influences on biogenic secondary organic aerosol formation. *Atmos. Chem. Phys.*, **19**, 3191-3206.

Hildebrandt, L., K. M. Henry, J. H. Kroll, D. R. Worsnop, S. N. Pandis, and N. M. Donahue, 2011: Evaluating the mixing of organic aerosol components using high-resolution aerosol mass spectrometry. *Environ. Sci. Technol.*, **45**, 6329-6335.

Ho, K. F., S. C. Lee, S. S. H. Ho, K. Kawamura, E. Tachibana, Y. Cheng, and T. Zhu, 2010: Dicarboxylic acids, ketocarboxylic acids, α-dicarbonyls, fatty acids, and benzoic acid in urban aerosols collected during the 2006 Campaign of Air Quality Research in Beijing (CAREBeijing-2006). *J. Geophys. Res.*, **115**, D19312.

Hodzic, A., P. S. Kasibhatla, D. S. Jo, C. D. Cappa, J. L. Jimenez, S. Madronich, and R. J. Park, 2016: Rethinking the global secondary organic aerosol (SOA) budget:

stronger production, faster removal, shorter lifetime. *Atmos. Chem. Phys.*, **16**, 7917-7941.

Hoesly, R. M., and Coauthors, 2018: Historical (1750–2014) anthropogenic emissions of reactive gases and aerosols from the Community Emissions Data System (CEDS). *Geosci. Model Dev.*, **11**, 369-408.

Hoyle, C. R., G. Myhre, T. K. Berntsen, and I. S. A. Isaksen, 2009: Anthropogenic influence on SOA and the resulting radiative forcing. *Atmos. Chem. Phys.*, **9**, 2715-2728.

Hoyle, C. R., and Coauthors, 2011: A review of the anthropogenic influence on biogenic secondary organic aerosol. *Atmos. Chem. Phys.*, **11**, 321-343.

Hu, J. L., and Coauthors, 2017: Modeling biogenic and anthropogenic secondary organic aerosol in China. *Atmos. Chem. Phys.*, **17**, 77-92.

Huang, H.-L., W. Chao, and J. J.-M. Lin, 2015: Kinetics of a Criegee intermediate that would survive high humidity and may oxidize atmospheric SO_2. *Proc. Natl. Acad. Sci. U.S.A.*, **112**, 10857-10862.

Huang, R. J., and Coauthors, 2014: High secondary aerosol contribution to particulate pollution during haze events in China. *Nature*, **514**, 218-222.

Huang, W., H. Saathoff, X. Shen, R. Ramisetty, T. Leisner, and C. Mohr, 2019: Chemical characterization of highly functionalized organonitrates contributing to night-time organic aerosol mass loadings and particle growth. *Environ. Sci. Technol.*, **53**, 1165-1174.

Huang, Y., S. C. Lee, K. F. Ho, S. S. H. Ho, N. Cao, Y. Cheng, and Y. Gao, 2012: Effect of ammonia on ozone-initiated formation of indoor secondary products with emissions from cleaning products. *Atmos. Environ.*, **59**, 224-231.

Iinuma, Y., O. Böge, T. Gnauk, and H. Herrmann, 2004: Aerosol-chamber study of the

α-pinene/O_3 reaction: influence of particle acidity on aerosol yields and products. *Atmos. Environ.*, **38**, 761-773.

Iinuma, Y., A. Kahnt, A. Mutzel, O. Boge, and H. Herrmann, 2013: Ozone-driven secondary organic aerosol production chain. *Environ. Sci. Technol.*, **47**, 3639-3647.

Jang, M. S., N. M. Czoschke, S. Lee, and R. M. Kamens, 2002: Heterogeneous atmospheric aerosol production by acid-catalyzed particle-phase reactions. *Science*, **298**, 814-817.

Jaoui, M., T. E. Kleindienst, K. S. Docherty, M. Lewandowski, and J. H. Offenberg, 2013: Secondary organic aerosol formation from the oxidation of a series of sesquiterpenes: α-cedrene, β-caryophyllene, α-humulene and α-farnesene with O_3, OH and NO_3 radicals. *Environ. Chem.*, **10**, 178-193.

Jathar, S. H., C. D. Cappa, A. S. Wexler, J. H. Seinfeld, and M. J. Kleeman, 2016: Simulating secondary organic aerosol in a regional air quality model using the statistical oxidation model - Part 1: Assessing the influence of constrained multi-generational ageing. *Atmos. Chem. Phys.*, **16**, 2309-2322.

Jiang, J. H., and Coauthors, 2019: Sources of organic aerosols in Europe: a modeling study using CAMx with modified volatility basis set scheme. *Atmos. Chem. Phys.*, **19**, 15247-15270.

Kawamura, K., and S. Bikkina, 2016: A review of dicarboxylic acids and related compounds in atmospheric aerosols: Molecular distributions, sources and transformation. *Atmos. Res.*, **170**, 140-160.

Kelly, J. M., R. M. Doherty, amp, apos, F. M. Connor, and G. W. Mann, 2018: The impact of biogenic, anthropogenic, and biomass burning volatile organic compound emissions on regional and seasonal variations in secondary organic aerosol. *Atmos. Chem. Phys.*, **18**, 7393-7422.

Kiendler-Scharr, A., and Coauthors, 2016: Ubiquity of organic nitrates from nighttime chemistry in the European submicron aerosol. *Geophys. Res. Lett.*, **43**, 7735-7744.

Kim, H., B. Barkey, and S. E. Paulson, 2010: Real refractive indices of α- and β-pinene and toluene secondary organic aerosols generated from ozonolysis and photo-oxidation. *J. Geophys. Res. Atmos.*, **115**, D24212.

Kim, H., B. Barkey, and S. E. Paulson, 2012: Real refractive indices and formation yields of secondary organic aerosol generated from photooxidation of limonene and alpha-pinene: the effect of the HC/NO(x) ratio. *J. Phys. Chem. A*, **116**, 6059-6067.

King, S. M., and Coauthors, 2010: Cloud droplet activation of mixed organic-sulfate particles produced by the photooxidation of isoprene. *Atmos. Chem. Phys.*, **10**, 3953-3964.

Kleindienst, T. E., E. O. Edney, M. Lewandowski, J. H. Offenberg, and M. Jaoui, 2006: Secondary organic carbon and aerosol yields from the irradiations of isoprene and α-pinene in the presence of NOx and SO_2. *Environ. Sci. Technol.*, **40**, 3807-3812.

Kourtchev, I., and Coauthors, 2014: Effects of anthropogenic emissions on the molecular composition of urban organic aerosols: An ultrahigh resolution mass spectrometry study. *Atmos. Environ.*, **89**, 525-532.

Kristensen, K., T. Cui, H. Zhang, A. Gold, M. Glasius, and J. D. Surratt, 2014: Dimers in α-pinene secondary organic aerosol: effect of hydroxyl radical, ozone, relative humidity and aerosol acidity. *Atmos. Chem. Phys.*, **14**, 4201-4218.

Kroll, J. H., and J. H. Seinfeld, 2008: Chemistry of secondary organic aerosol: Formation and evolution of low-volatility organics in the atmosphere. *Atmos. Environ.*, **42**, 3593-3624.

Kroll, J. H., N. L. Ng, S. M. Murphy, R. C. Flagan, and J. H. Seinfeld, 2005: Secondary organic aerosol formation from isoprene photooxidation under high-NOx conditions.

Geophys. Res. Lett., **32**, L18808.

Kroll, J. H., N. L. Ng, S. M. Murphy, R. C. Flagan, and J. H. Seinfeld, 2006: Secondary organic aerosol formation from isoprene photooxidation. *Environ. Sci. Technol.*, **40**, 1869-1877.

La, Y. S., and Coauthors, 2016: Impact of chamber wall loss of gaseous organic compounds on secondary organic aerosol formation: explicit modeling of SOA formation from alkane and alkene oxidation. *Atmos. Chem. Phys.*, **16**, 1417-1431.

Laskin, J., and Coauthors, 2010: High-resolution desorption electrospray ionization mass spectrometry for chemical characterization of organic aerosols. *Anal. Chem.*, **82**, 2048-2058.

Laskin, J., and Coauthors, 2014: Molecular selectivity of brown carbon chromophores. *Environ. Sci. Technol.*, **48**, 12047-12055.

Lee, A., A. H. Goldstein, J. H. Kroll, N. L. Ng, V. Varutbangkul, R. C. Flagan, and J. H. Seinfeld, 2006: Gas-phase products and secondary aerosol yields from the photooxidation of 16 different terpenes. *J. Geophys. Res.*, **111**, D17305.

Lee, H. J., A. Laskin, J. Laskin, and S. A. Nizkorodov, 2013: Excitation-emission spectra and fluorescence quantum yields for fresh and aged biogenic secondary organic aerosols. *Environ. Sci. Technol.*, **47**, 5763-5770.

Lee, H. J., P. K. Aiona, A. Laskin, J. Laskin, and S. A. Nizkorodov, 2014: Effect of solar radiation on the optical properties and molecular composition of laboratory proxies of atmospheric brown carbon. *Environ. Sci. Technol.*, **48**, 10217-10226.

Lee, J. W., and Coauthors, 2012: The effect of humidity on the ozonolysis of unsaturated compounds in aerosol particles. *Phys. Chem. Chem. Phys.*, **14**, 8023-8031.

Lelieveld, J., J. S. Evans, M. Fnais, D. Giannadaki, and A. Pozzer, 2015: The contribution of outdoor air pollution sources to premature mortality on a global scale.

Nature, **525**, 367-371.

Li, H. Y., and Coauthors, 2017a: Wintertime aerosol chemistry and haze evolution in an extremely polluted city of the North China Plain: significant contribution from coal and biomass combustion. *Atmos. Chem. Phys.*, **17**, 4751-4768.

Li, J. J., and Coauthors, 2013: Abundance, composition and source of atmospheric PM2.5 at a remote site in the Tibetan Plateau, China. *Tellus B*, **65**, 20281.

Li, S. M., and Coauthors, 2017b: Differences between measured and reported volatile organic compound emissions from oil sands facilities in Alberta, Canada. *Proc. Natl. Acad. Sci. U.S.A.*, **114**, E3756-E3765.

Liao, H., W. Chang, and Y. Yang, 2014: Climatic effects of air pollutants over china: A review. *Adv. Atmos. Sci.*, **32**, 115-139.

Lim, H. J., A. G. Carlton, and B. J. Turpin, 2005: Isoprene forms secondary organic aerosol through cloud processing: Model simulations. *Environ. Sci. Technol.*, **39**, 4441-4446.

Lin, G., S. Sillman, J. E. Penner, and A. Ito, 2014: Global modeling of SOA: the use of different mechanisms for aqueous-phase formation. *Atmos. Chem. Phys.*, **14**, 5451-5475.

Lin, Y. H., E. M. Knipping, E. S. Edgerton, S. L. Shaw, and J. D. Surratt, 2013a: Investigating the influences of SO_2 and NH_3 levels on isoprene-derived secondary organic aerosol formation using conditional sampling approaches. *Atmos. Chem. Phys.*, **13**, 8457-8470.

Lin, Y. H., and Coauthors, 2012: Isoprene epoxydiols as precursors to secondary organic aerosol formation: acid-catalyzed reactive uptake studies with authentic compounds. *Environ. Sci. Technol.*, **46**, 250-258.

Lin, Y. H., and Coauthors, 2013b: Epoxide as a precursor to secondary organic aerosol

formation from isoprene photooxidation in the presence of nitrogen oxides. *Proc. Natl. Acad. Sci. U.S.A.*, **110**, 6718-6723.

Liu, J., and Coauthors, 2016: Efficient isoprene secondary organic aerosol formation from a non-IEPOX pathway. *Environ. Sci. Technol.*, **50**, 9872-9880.

Liu, J., and Coauthors, 2018: Regional similarities and NOx-related increases in biogenic secondary organic aerosol in summertime southeastern United States. *J. Geophys. Res. Atmos.*, **123**, 10620-10636.

Liu, M., and Coauthors, 2019: Ammonia emission control in China would mitigate haze pollution and nitrogen deposition, but worsen acid rain. *Proc. Natl. Acad. Sci. U.S.A.*, **116**, 7760-7765.

Liu, S., L. Jia, Y. Xu, N. T. Tsona, S. Ge, and L. Du, 2017: Photooxidation of cyclohexene in the presence of SO_2: SOA yield and chemical composition. *Atmos. Chem. Phys.*, **17**, 13329-13343.

Liu, Y., Q. Ma, and H. He, 2012: Heterogeneous uptake of amines by citric acid and humic acid. *Environ. Sci. Technol.*, **46**, 11112-11118.

Liu, Y., J. Liggio, R. Staebler, and S. M. Li, 2015: Reactive uptake of ammonia to secondary organic aerosols: Kinetics of organonitrogen formation. *Atmos. Chem. Phys.*, **15**, 13569-13584.

Loza, C. L., M. M. Coggon, T. B. Nguyen, A. Zuend, R. C. Flagan, and J. H. Seinfeld, 2013: On the mixing and evaporation of secondary organic aerosol components. *Environ. Sci. Technol.*, **47**, 6173-6180.

Lu, M., and Coauthors, 2019: Investigating the Transport Mechanism of PM2.5 Pollution during January 2014 in Wuhan, Central China. *Adv. Atmos. Sci.*, **36**, 1217-1234.

Ma, J. Z., X. B. Xu, C. S. Zhao, and P. Yan, 2012: A review of atmospheric chemistry

research in China: Photochemical smog, haze pollution, and gas-aerosol interactions. *Adv. Atmos. Sci.*, **29**, 1006-1026.

Ma, Q., X. Lin, C. Yang, B. Long, Y. Gai, and W. Zhang, 2018: The influences of ammonia on aerosol formation in the ozonolysis of styrene: Roles of Criegee intermediate reactions. *R. Soc. Open Sci.*, **5**, 172171.

Mackenzie-Rae, F. A., H. J. Wallis, A. R. Rickard, K. L. Pereira, S. M. Saunders, X. Wang, and J. F. Hamilton, 2018: Ozonolysis of α-phellandrene – Part 2: Compositional analysis of secondary organic aerosol highlights the role of stabilised Criegee intermediates. *Atmos. Chem. Phys.*, **18**, 4673-4693.

Marais, E. A., D. J. Jacob, J. R. Turner, and L. J. Mickley, 2017: Evidence of 1991–2013 decrease of biogenic secondary organic aerosol in response to SO_2 emission controls. *Environ. Res. Lett.*, **12**, 054018.

Matsui, H., M. Koike, Y. Kondo, A. Takami, J. D. Fast, Y. Kanaya, and M. Takigawa, 2014: Volatility basis-set approach simulation of organic aerosol formation in East Asia: implications for anthropogenic-biogenic interaction and controllable amounts. *Atmos. Chem. Phys.*, **14**, 9513-9535.

Mauldin III, R. L., and Coauthors, 2012: A new atmospherically relevant oxidant of sulphur dioxide. *Nature*, **488**, 193-196.

May, A. A., and Coauthors, 2013: Gas-particle partitioning of primary organic aerosol emissions: 3. Biomass burning. *J. Geophys. Res. Atmos.*, **118**, 11327-11338.

Meng, J., and Coauthors, 2014: Seasonal characteristics of oxalic acid and related SOA in the free troposphere of Mt. Hua, central China: implications for sources and formation mechanisms. *Sci Total Environ*, **493**, 1088-1097.

Meng, Z., and Coauthors, 2018: Role of ambient ammonia in particulate ammonium formation at a rural site in the North China Plain. *Atmos. Chem. Phys.*, **18**, 167-184.

Moise, T., J. M. Flores, and Y. Rudich, 2015: Optical properties of secondary organic aerosols and their changes by chemical processes. *Chem. Rev.*, **115**, 4400-4439.

Na, K., C. Song, and D. Cockeriii, 2006: Formation of secondary organic aerosol from the reaction of styrene with ozone in the presence and absence of ammonia and water. *Atmos. Environ.*, **40**, 1889-1900.

Na, K., C. Song, C. Switzer, and D. R. Cocker, 2007: Effect of ammonia on secondary organic aerosol formation from α-pinene ozonolysis in dry and humid conditions. *Environ. Sci. Technol.*, **41**, 6096-6102.

Newland, M. J., and Coauthors, 2018: The atmospheric impacts of monoterpene ozonolysis on global stabilised Criegee intermediate budgets and SO_2 oxidation: experiment, theory and modelling. *Atmos. Chem. Phys.*, **18**, 6095-6120.

Ng, N. L., J. H. Kroll, A. W. H. Chan, P. S. Chhabra, R. C. Flagan, and J. H. Seinfeld, 2007a: Secondary organic aerosol formation from m-xylene, toluene, and benzene. *Atmos. Chem. Phys.*, **7**, 3909-3922.

Ng, N. L., and Coauthors, 2007b: Effect of NOx level on secondary organic aerosol (SOA) formation from the photooxidation of terpenes. *Atmos. Chem. Phys.*, **7**, 5159-5174.

Ng, N. L., and Coauthors, 2017: Nitrate radicals and biogenic volatile organic compounds: oxidation, mechanisms, and organic aerosol. *Atmos. Chem. Phys.*, **17**, 2103-2162.

Nguyen, T. B., and Coauthors, 2014: Organic aerosol formation from the reactive uptake of isoprene epoxydiols (IEPOX) onto non-acidified inorganic seeds. *Atmos. Chem. Phys.*, **14**, 3497-3510.

Nguyen, T. B., and Coauthors, 2015: Mechanism of the hydroxyl radical oxidation of methacryloyl peroxynitrate (MPAN) and its pathway toward secondary organic aerosol

formation in the atmosphere. *Phys. Chem. Chem. Phys.*, **17**, 17914-17926.

Niu, X., and Coauthors, 2017: Indoor secondary organic aerosols formation from ozonolysis of monoterpene: An example of d-limonene with ammonia and potential impacts on pulmonary inflammations. *Sci. Total. Environ.*, **579**, 212-220.

Nøjgaard, J. K., M. Bilde, C. Stenby, O. J. Nielsen, and P. Wolkoff, 2006: The effect of nitrogen dioxide on particle formation during ozonolysis of two abundant monoterpenes indoors. *Atmos. Environ.*, **40**, 1030-1042.

Odum, J. R., T. Hoffmann, F. Bowman, D. Collins, R. C. Flagan, and J. H. Seinfeld, 1996: Gas/particle partitioning and secondary organic aerosol yields. *Environ. Sci. Technol.*, **30**, 2580-2585.

Offenberg, J. H., M. Lewandowski, E. O. Edney, T. E. Kleindienst, and M. Jaoui, 2009: Influence of aerosol acidity on the formation of secondary organic aerosol from biogenic precursor hydrocarbons. *Environ. Sci. Technol.*, **43**, 7742-7747.

Pandis, S. N., S. E. Paulson, J. H. Seinfeld, and R. C. Flagan, 1991: Aerosol formation in the photooxidation of isoprene and β-pinene. *Atmos. Environ., Part A*, **25**, 997-1008.

Pankow, J. F., 1994a: An absorption-model of gas-particle partitioning of organic-compounds in the atmosphere. *Atmos. Environ.*, **28**, 185-188.

Pankow, J. F., 1994b: An absorption-model of the gas aerosol partitioning involved in the formation of secondary organic aerosol. *Atmos. Environ.*, **28**, 189-193.

Perraud, V., and Coauthors, 2012: Nonequilibrium atmospheric secondary organic aerosol formation and growth. *Proc. Natl. Acad. Sci. U.S.A.*, **109**, 2836-2841.

Presto, A. A., K. E. Hartz, and N. M. Donahue, 2005: Secondary Organic Aerosol production from terpene ozonolysis. 2. Effect of NOx concentration. *Environ. Sci. Technol.*, **39**, 7046-7054.

Pye, H. O., and Coauthors, 2013: Epoxide pathways improve model predictions of

isoprene markers and reveal key role of acidity in aerosol formation. *Environ. Sci. Technol.*, **47**, 11056-11064.

Qin, M., and Coauthors, 2018a: Simulating biogenic secondary organic aerosol during summertime in China. *J. Geophys. Res. Atmos.*, **123**, 11100-11119.

Qin, M., and Coauthors, 2018b: Modeling biogenic secondary organic aerosol (BSOA) formation from monoterpene reactions with NO_3: A case study of the SOAS campaign using CMAQ. *Atmos. Environ.*, **184**, 146-155.

Qiu, C., and R. Zhang, 2013: Multiphase chemistry of atmospheric amines. *Phys. Chem. Chem. Phys.*, **15**, 5738-5752.

Rattanavaraha, W., and Coauthors, 2017: Assessing the impact of anthropogenic pollution on isoprene-derived secondary organic aerosol formation in PM2.5 collected from the Birmingham, Alabama, ground site during the 2013 Southern Oxidant and Aerosol Study. *Atmos. Chem. Phys.*, **16**, 4897-4914.

Ren, Y., and Coauthors, 2018: Seasonal variation and size distribution of biogenic secondary organic aerosols at urban and continental background sites of China. *J Environ Sci (China)*, **71**, 32-44.

Ren, Y., and Coauthors, 2019: Seasonal characteristics of biogenic secondary organic aerosols at Mt. Wuyi in Southeastern China: Influence of anthropogenic pollutants. *Environ Pollut*, **252**, 493-500.

Riipinen, I., T. Yli-Juuti, J. R. Pierce, T. Petaja, D. R. Worsnop, M. Kulmala, and N. M. Donahue, 2012: The contribution of organics to atmospheric nanoparticle growth. *Nat. Geosci.*, **5**, 453-458.

Riva, M., S. H. Budisulistiorini, Z. Zhang, A. Gold, and J. D. Surratt, 2016a: Chemical characterization of secondary organic aerosol constituents from isoprene ozonolysis in the presence of acidic aerosol. *Atmos. Environ.*, **130**, 5-13.

Riva, M., and Coauthors, 2016b: Effect of organic coatings, humidity and aerosol acidity on multiphase chemistry of isoprene epoxydiols. *Environ. Sci. Technol.*, **50**, 5580-5588.

Riva, M., and Coauthors, 2016c: Chemical characterization of secondary organic aerosol from oxidation of isoprene hydroxyhydroperoxides. *Environ. Sci. Technol.*, **50**, 9889-9899.

Robinson, E. S., R. Saleh, and N. M. Donahue, 2013: Organic aerosol mixing observed by single-particle mass spectrometry. *J. Phys. Chem. A*, **117**, 13935-13945.

Robinson, E. S., R. Saleh, and N. M. Donahue, 2015: Probing the evaporation dynamics of mixed SOA/squalane particles using size-resolved composition and single-particle measurements. *Environ. Sci. Technol.*, **49**, 9724-9732.

Rollins, A. W., and Coauthors, 2012: Evidence for NOx Control over Nighttime SOA Formation. *Science*, **337**, 1210-1212.

Saathoff, H., and Coauthors, 2009: Temperature dependence of yields of secondary organic aerosols from the ozonolysis of α-pinene and limonene. *Atmos. Chem. Phys.*, **9**, 1551-1577.

Sareen, N., S. G. Moussa, and V. F. McNeill, 2013: Photochemical aging of light-absorbing secondary organic aerosol material. *J. Phys. Chem. A*, **117**, 2987-2996.

Sarrafzadeh, M., and Coauthors, 2016: Impact of NOx and OH on secondary organic aerosol formation from β-pinene photooxidation. *Atmos. Chem. Phys.*, **16**, 11237-11248.

Shi, G., and Coauthors, 2017: pH of aerosols in a polluted atmosphere: source contributions to highly acidic aerosol. *Environ. Sci. Technol.*, **51**, 4289-4296.

Shrivastava, M., and Coauthors, 2017: Recent advances in understanding secondary organic aerosol: Implications for global climate forcing. *Rev. Geophys.*, **55**, 509-559.

Sipila, M., and Coauthors, 2014: Reactivity of stabilized Criegee intermediates (sCIs) from isoprene and monoterpene ozonolysis toward SO_2 and organic acids. *Atmos. Chem. Phys.*, **14**, 12143-12153.

Slade, J. H., and Coauthors, 2019: Bouncier particles at night: biogenic secondary organic aerosol chemistry and sulfate drive diel variations in the aerosol phase in a mixed forest. *Environ. Sci. Technol.*, **53**, 4977-4987.

Smith, S. J., H. Pitcher, and T. M. L. Wigley, 2001: Global and regional anthropogenic sulfur dioxide emissions. *Global Planet. Change*, **29**, 99-119.

Song, C., and Coauthors, 2007: Effect of hydrophobic primary organic aerosols on secondary organic aerosol formation from ozonolysis of α-pinene. *Geophys. Res. Lett.*, **34**, L20803.

Stangl, C. M., J. M. Krasnomowitz, M. J. Apsokardu, L. Tiszenkel, Q. Ouyang, S. Lee, and M. V. Johnston, 2019: Sulfur dioxide modifies aerosol particle formation and growth by ozonolysis of monoterpenes and isoprene. *J. Geophys. Res. Atmos.*, **124**, 4800-4811.

Stirnweis, L., and Coauthors, 2017: Assessing the influence of NOx concentrations and relative humidity on secondary organic aerosol yields from α-pinene photo-oxidation through smog chamber experiments and modelling calculations. *Atmos. Chem. Phys.*, **17**, 5035-5061.

Surratt, J. D., M. Lewandowski, J. H. Offenberg, M. Jaoui, T. E. Kleindienst, E. O. Edney, and J. H. Seinfeld, 2007: Effect of acidity on secondary organic aerosol formation from isoprene. *Environ. Sci. Technol.*, **41**, 5363-5369.

Surratt, J. D., and Coauthors, 2010: Reactive intermediates revealed in secondary organic aerosol formation from isoprene. *Proc. Natl. Acad. Sci. U.S.A.*, **107**, 6640-6645.

Tao, J., and Coauthors, 2013: Chemical composition of PM2.5 at an urban site of

Chengdu in southwestern China. *Adv. Atmos. Sci.*, **30**, 1070-1084.

Tasoglou, A., and S. N. Pandis, 2015: Formation and chemical aging of secondary organic aerosol during the β-caryophyllene oxidation. *Atmos. Chem. Phys.*, **15**, 6035-6046.

Tsimpidi, A. P., V. A. Karydis, S. N. Pandis, and J. Lelieveld, 2016: Global combustion sources of organic aerosols: model comparison with 84 AMS factor-analysis data sets. *Atmos. Chem. Phys.*, **16**, 8939-8962.

Updyke, K. M., T. B. Nguyen, and S. A. Nizkorodov, 2012: Formation of brown carbon via reactions of ammonia with secondary organic aerosols from biogenic and anthropogenic precursors. *Atmos. Environ.*, **63**, 22-31.

Vaden, T. D., C. Song, R. A. Zaveri, D. Imre, and A. Zelenyuk, 2010: Morphology of mixed primary and secondary organic particles and the adsorption of spectator organic gases during aerosol formation. *Proc. Natl. Acad. Sci. U.S.A.*, **107**, 6658-6663.

Vereecken, L., D. R. Glowacki, and M. J. Pilling, 2015: Theoretical chemical kinetics in tropospheric chemistry: methodologies and applications. *Chem. Rev.*, **115**, 4063-4114.

von Schneidemesser, E., and Coauthors, 2015: Chemistry and the linkages between air Quality and climate change. *Chem. Rev.*, **115**, 3856-3897.

Wang, G., C. Cheng, J. Meng, Y. Huang, J. Li, and Y. Ren, 2015: Field observation on secondary organic aerosols during Asian dust storm periods: Formation mechanism of oxalic acid and related compounds on dust surface. *Atmos. Environ.*, **113**, 169-176.

Wang, G., and Coauthors, 2012: Molecular distribution and stable carbon isotopic composition of dicarboxylic acids, ketocarboxylic acids, and α-dicarbonyls in size-resolved atmospheric particles from Xi'an City, China. *Environ. Sci. Technol.*, **46**, 4783-4791.

Wang, H., and Coauthors, 2020a: NO_3 and N_2O_5 chemistry at a suburban site during the EXPLORE-YRD campaign in 2018. *Atmos. Environ.*, **224**, 117180.

Wang, Q., and Coauthors, 2020b: Seasonal characterization of aerosol composition and sources in a polluted city in Central China. *Chemosphere*, **258**, 127310.

Wang, S., and Coauthors, 2019: Organic Peroxides and Sulfur Dioxide in Aerosol: Source of Particulate Sulfate. *Environ. Sci. Technol.*, **53**, 10695-10704.

Wang, W., and Coauthors, 2008: Polar organic tracers in PM2.5 aerosols from forests in eastern China. *Atmos. Chem. Phys.*, **8**, 7507-7518.

Wang, X., and Coauthors, 2013: Size distributions of aerosol sulfates and nitrates in Beijing during the 2008 Olympic Games: Impacts of pollution control measures and regional transport. *Adv. Atmos. Sci.*, **30**, 341-353.

Warner, J. X., R. R. Dickerson, Z. Wei, L. L. Strow, Y. Wang, and Q. Liang, 2017: Increased atmospheric ammonia over the world's major agricultural areas detected from space. *Geophys. Res. Lett.*, **44**, 2875-2884.

Wayne, R. P., and Coauthors, 1991: The nitrate radical: Physics, chemistry, and the atmosphere. *Atmos. Environ., Part A*, **25**, 1-203.

Weber, R. J., H. Guo, A. G. Russell, and A. Nenes, 2016: High aerosol acidity despite declining atmospheric sulfate concentrations over the past 15 years. *Nat. Geosci.*, **9**, 282-285.

Wildt, J., and Coauthors, 2014: Suppression of new particle formation from monoterpene oxidation by NOx. *Atmos. Chem. Phys.*, **14**, 2789-2804.

Worton, D. R., and Coauthors, 2013: Observational insights into aerosol formation from isoprene. *Environ. Sci. Technol.*, **47**, 11403-11413.

Wu, K., and Coauthors, 2020: Estimation of biogenic VOC emissions and their corresponding impact on ozone and secondary organic aerosol formation in China.

Atmos. Res., **231**, 104656.

Xia, Y., Z. Yu, and C. P. Nielsen, 2016: Benefits of China's efforts in gaseous pollutant control indicated by the bottom-up emissions and satellite observations 2000-2014. *Atmos. Environ.*, **136**, 43-53.

Xing, L., and Coauthors, 2019: Wintertime secondary organic aerosol formation in Beijing–Tianjin–Hebei (BTH): contributions of HONO sources and heterogeneous reactions. *Atmos. Chem. Phys.*, **19**, 2343-2359.

Xu, L., M. S. Kollman, C. Song, J. E. Shilling, and N. L. Ng, 2014: Effects of NOx on the volatility of secondary organic aerosol from isoprene photooxidation. *Environ. Sci. Technol.*, **48**, 2253-2262.

Xu, L., S. Suresh, H. Guo, R. J. Weber, and N. L. Ng, 2015a: Aerosol characterization over the southeastern United States using high-resolution aerosol mass spectrometry: spatial and seasonal variation of aerosol composition and sources with a focus on organic nitrates. *Atmos. Chem. Phys.*, **15**, 7307-7336.

Xu, L., H. O. T. Pye, J. He, Y. Chen, B. N. Murphy, and L. N. Ng, 2018: Experimental and model estimates of the contributions from biogenic monoterpenes and sesquiterpenes to secondary organic aerosol in the southeastern United States. *Atmos. Chem. Phys.*, **18**, 12613-12637.

Xu, L., and Coauthors, 2020: NOx enhances secondary organic aerosol formation from nighttime γ-terpinene ozonolysis. *Atmos. Environ.*, **225**, 117375.

Xu, L., and Coauthors, 2015b: Effects of anthropogenic emissions on aerosol formation from isoprene and monoterpenes in the southeastern United States. *Proc. Natl. Acad. Sci. U.S.A.*, **112**, 37-42.

Ye, J., J. P. D. Abbatt, and A. W. H. Chan, 2018: Novel pathway of SO_2 oxidation in the atmosphere: Reactions with monoterpene ozonolysis intermediates and secondary

organic aerosol. *Atmos. Chem. Phys.*, **18**, 5549-5565.

Yee, L. D., and Coauthors, 2020: Natural and anthropogenically influenced isoprene oxidation in southeastern United States and central Amazon. *Environ. Sci. Technol.*, **54**, 5980-5991.

Yu, J. Z., X. F. Huang, J. H. Xu, and M. Hu, 2005: When aerosol sulfate goes up, so does oxalate: Implication for the formation mechanisms of oxalate. *Environ. Sci. Technol.*, **39**, 128-133.

Yu, K. Y., Q. Zhu, K. Du, and X. F. Huang, 2019: Characterization of nighttime formation of particulate organic nitrates based on high-resolution aerosol mass spectrometry in an urban atmosphere in China. *Atmos. Chem. Phys.*, **19**, 5235-5249.

Zeng, Y., S. Tian, and Y. Pan, 2018: Revealing the sources of atmospheric ammonia: a review. *Curr. Pollut. Rep.*, **4**, 189-197.

Zhang, H., J. D. Surratt, Y. H. Lin, J. Bapat, and R. M. Kamens, 2011: Effect of relative humidity on SOA formation from isoprene/NO photooxidation: enhancement of 2-methylglyceric acid and its corresponding oligoesters under dry conditions. *Atmos. Chem. Phys.*, **11**, 6411-6424.

Zhang, H., and Coauthors, 2018: Monoterpenes are the largest source of summertime organic aerosol in the southeastern United States. *Proc. Natl. Acad. Sci. U.S.A.*, **115**, 2038-2043.

Zhang, J., Y. Wang, X. Huang, Z. Liu, D. Ji, and Y. Sun, 2015a: Characterization of organic aerosols in Beijing using an aerodyne high-resolution aerosol mass spectrometer. *Adv. Atmos. Sci.*, **32**, 877-888.

Zhang, J., and Coauthors, 2017a: Chemical composition, source, and process of urban aerosols during winter haze formation in Northeast China. *Environ. Pollut.*, **231**, 357-366.

Zhang, P., and Coauthors, 2019a: Impacts of SO_2, relative humidity, and seed acidity on secondary organic aerosol formation in the ozonolysis of butyl vinyl ether. *Environ. Sci. Technol.*, **53**, 8845-8853.

Zhang, R., and Coauthors, 2015b: Formation of urban fine particulate matter. *Chem. Rev.*, **115**, 3803-3855.

Zhang, S. H., M. Shaw, J. H. Seinfeld, and R. C. Flagan, 1992: Photochemical aerosol formation from α-pinene- and β-pinene *J. Geophys. Res. Atmos.*, **97**, 20717-20729.

Zhang, Y., and Coauthors, 2017b: High contribution of nonfossil sources to submicrometer organic aerosols in Beijing, China. *Environ. Sci. Technol.*, **51**, 7842-7852.

Zhang, Y. J., and Coauthors, 2017c: Limited formation of isoprene epoxydiols-derived secondary organic aerosol under NOx-rich environments in Eastern China. *Geophys. Res. Lett.*, **44**, 2035-2043.

Zhang, Y. Q., and Coauthors, 2019b: Impact of anthropogenic emissions on biogenic secondary organic aerosol: Observation in the Pearl River Delta, southern China. *Atmos. Chem. Phys.*, **19**, 14403-14415.

Zhao, C., Y. Li, F. Zhang, Y. Sun, and P. Wang, 2018a: Growth rates of fine aerosol particles at a site near Beijing in June 2013. *Adv. Atmos. Sci.*, **35**, 209-217.

Zhao, D., and Coauthors, 2018b: Effects of NOx and SO_2 on the secondary organic aerosol formation from photooxidation of α-pinene and limonene. *Atmos. Chem. Phys.*, **18**, 1611-1628.

Zhao, Z., Q. Xu, X. Yang, and H. Zhang, 2019: Heterogeneous ozonolysis of endocyclic unsaturated organic aerosol proxies: Implications for Criegee intermediate dynamics and later-generation reactions. *ACS Earth Space Chem.*, **3**, 344-356.

Zhu, B., H. Wang, L. Shen, H. Kang, and X. Yu, 2013: Aerosol spectra and new particle

formation observed in various seasons in Nanjing. *Adv. Atmos. Sci.*, **30**, 1632-1644.

Ziemann, P. J., and R. Atkinson, 2012: Kinetics, products, and mechanisms of secondary organic aerosol formation. *Chem. Soc. Rev.*, **41**, 6582-6605.

Table 1. SOA formation from BVOCs photooxidation in the presence of NOx.

BVOCs	$[BVOC]_0$ (ppb)	$[NOx]_0/[BVOC]_0$	·OH precursors	T (K)	RH (%)	Seed	SOA mass (μg m^{-3})	Yield (%)	Notes	References
isoprene	91.4-114.6	0.7-7.3	H_2O_2	~298	< 5	none	4.2-30.2	1.5-8.5	The SOA yield increased with initial NO/isoprene up to a ratio of 3, beyond which it decreases with increasing initial $[NO]_0/[isoprene]_0$ ratio.	(Xu et al., 2014)
	45±4	0-17	H_2O_2	~301	< 10	ammonium sulfate	1.7-6.7	1.4-5.5	At high NOx (>200 ppb), the SOA yield decreased with increasing NOx.	(Kroll et al., 2006)
	26	0-1.9	H_2O_2	-	50	ammonium sulfate	1.9-7.6	2.7-11.6	The SOA yield was nearly constant at low NO until the $[NO]_0/[isoprene]_0$ ratio reached ~0.38). It further decreased with the increase of NO concentrations.	(Liu et al., 2016)
	50	0-0.5	H_2O_2	~298	40±2	ammonium sulfate	0.5-1.2	0. 4-0.9	Higher $[NOx]_0/[isoprene]_0$ ratios produced lower aerosol yields.	(King et al., 2010)
	33-523	1.6-32	CH_3ONO/HONO	296-298	9-11	ammonium sulfate	2.9-65.2	3.1-7.4	SOA yields were relevant to NO_2/NO ratio under high NOx conditions.	(Chan et al., 2010)
	25-500	0.5-7.6	HONO	293-295	42-50	ammonium sulfate	0.7.-42.6	0.9–3	Higher $[NOx]_0/[isoprene]_0$ ratios produced lower aerosol yields.	(Kroll et al., 2005)
	180-2500	0.2-0.7	NOx	293	47-53	none	0.7–336	0.2-5.3	SOA yields first increased ($[NOx]_0/[isoprene]_0$ < 0.5) and then decreased with $[NOx]_0/[isoprene]_0$ ($[NOx]_0/[isoprene]_0$ > 0 .5).	(Dommen et al., 2006)

α-pinene	~15	0-64.5	H_2O_2/HONO	296-299	3.3-6.4	ammonium sulfate	4.5-29.3	6.6-37.9	SOA yields were higher at lower initial $[NOx]_0/[\alpha\text{-pinene}]_0$ ratios.	(Ng et al., 2007b)
	18.3-20.3	0.1-2.6	HONO	294-299	27-29	ammonium hydrogen sulfate and sulfuric acid	2.1-12	1.8-11.6	The yields at low $[NOx]_0/[\alpha\text{-pinene}]_0$ ratios were in general higher compared to those at high $[NOx]_0/[\alpha\text{-pinene}]_0$.	(Stirnweis et al., 2017)
	16.1-20.7	1.2-3.8	HONO	294-299	66-69	ammonium hydrogen sulfate and sulfuric acid	8.6-13.4	8.1-13.8	The yields at low $[NOx]_0/[\alpha\text{-pinene}]_0$ ratios were in general higher compared to those at high $[NOx]_0/[\alpha\text{-pinene}]_0$.	(Stirnweis et al., 2017)
	45-52.4	-	H_2O_2/HONO/CH_3ONO	293-298	< 10	ammonium sulfate	37.2-76.6	14.4-28.9	The SOA yield was suppressed under conditions of high NO.	(Eddingsaas et al., 2012)
	65-120	0.3-1.2	NOx	306-315	14-17	none	18-136	5.3-24	Aerosol yields should be higher at lower $[NOx]_0/[\alpha\text{-pinene}]_0$ ratios.	(Kim et al., 2012)
	470-845	0.4-0.9	NOx	310-316	14-17	none	830-2100	34-68	SOA yields were higher at lower initial NOx/α-pinene ratios.	(Kim et al., 2010)
	~ 20	~ 0-1	HONO	291-307	29-42	none	-	0-10	Higher $[NOx]_0/[\alpha\text{-pinene}]_0$ ratios produced lower aerosol yields.	(Zhao et al., 2018b)
β-pinene	37	0.01-3.9	HO_2/NO	289±1	63±2	ammonium sulfate	14.3-38.1	8.2-20.0	SOA yields increased with increasing [NOx] at low-NOx conditions ($[NOx]_0$ < 30 ppb, $[NOx]_0/[\beta\text{-pinene}]_0$ < 1 and decreased with [NOx] at high-NOx conditions ($[NOx]_0$ >30 ppb, NOx/β-pinene ~1 to ~3.8).	(Sarrafzadeh et al., 2016)
	36-2000	0.2-19.6	NOx	-	-	none	-	-	Aerosol yields were small when $[NOx]_0/[\beta\text{-pinene}]_0$ was larger than 2, increased	(Pandis et al., 1991)

									dramatically and reached maximum for the range of 0.7-1, then decreased slowly as the ratio decrease.	
	405-640	0.4-0.9	NOx	312-317	12-19	none	430-900	25-37	Higher $[NOx]_0/[\beta\text{-pinene}]_0$ ratios produced lower aerosol yields.	(Kim et al., 2010)
	32.3-96.5[a]	~2-10	NOx	308-313	~5	ammonium sulfate	7.2-141.6	3.2-27.2	SOA yields were lower at higher NOx levels than at lower NOx levels.[b]	(Griffin et al., 1999)
limonene	60-75	0.3-1.6	NOx	304-312	14-21	none	79.2-136	27-40	Higher $[NOx]_0/[\text{limonene}]_0$ ratios produced lower aerosol yields.	(Kim et al., 2012)
	~ 7	~ 0-2.9	HONO	293-303	28-31	none	-	0-5	Higher $[NOx]_0/[\text{limonene}]_0$ ratios produced lower aerosol yields.	(Zhao et al., 2018b)
	20.6-65.1[a]	~2-5	NOx	309-313	~5	ammonium sulfate	9.5-120.2	8.7-34.4	SOA yields were lower at higher NOx levels than at lower NOx levels. [b]	(Griffin et al., 1999)
sabinene	13.9-83.3[a]	~2-10	NOx	310-316	~5	ammonium sulfate	2.5-14.5	1.9-65.2	SOA yields are lower at higher NOx levels than at lower NOx levels. [b]	(Griffin et al., 1999)
α-humulene	5-9.2[a]	~2-10	NOx	309-312	~5	ammonium sulfate	12.9-59.2	31.9-84.5	The yields dependence on NOx levels is not obvious. [b]	(Griffin et al., 1999)
longifolene	~4.3	0-131	H_2O_2/HONO	296-299	3.3-6.4	ammonium sulfate	28.5-51.6	84-157	SOA yields under high-NOx conditions exceed those under low-NOx conditions.	(Ng et al., 2007b)
aromadendrene	~5	0-~103	H_2O_2/HONO	296-299	3.3-6.4	ammonium sulfate	19.7-29.3	41.7-84.7	Aerosol yields increase with NOx concentrations.	(Ng et al., 2007b)
β-caryophyllene	3-32	0-1.7	H_2O_2/HONO	293±2	< 10	ammonium sulfate	8.4-311	19.3-137.8	SOA yields at low NOx conditions were lower than those at high NOx conditions.	(Tasoglou and Pandis, 2015)

	31.1-52.4	0.5-1.7	NOx	~298	~70	none	35.6-66.2	9.5-19.9	The yields dependence on NOx levels was not obvious.	(Alfarra et al., 2012)
	5.9-12.9	~2-5	NOx	309-312	~5	ammonium sulfate	17.6-82.3	13.1-39.0	The yields dependence on NOx levels was not obvious.	(Griffin et al., 1999)

[a] Mixing ratios of BVOCs reacted due to the unavailable initial BVOCs concentrations. [b] Effects of NOx on SOA yields are hypothesized if the reacted BVOCs are equal to the initial ones.

Table 2. SOA formation from BVOCs ozonolysis in the presence of NOx.

BVOCs	$[BVOC]_0$ (ppb)	$[NOx]_0/[BVOC]_0$	$[NOx]_0/[O_3]_0$	T (K)	RH (%)	Seed	SOA mass ($\mu g\ m^{-3}$)	Yield (%)	Notes	References
α-pinene	15-200	0.7-70	~0.03-4	288-313	-	none	1-346	0-0.29	The yields increase as NO_2 concentrations decrease and reach an asymptote near $[NOx]_0/[BVOC]_0 = 0.7$.	(Presto et al., 2005)
	300-960	~0-4.7	0-2.9	294-295	22-30	none	-	-	The increase of $[NO_2]_0$ substantially depletes SOA formation.	(Draper et al., 2015)
	1000	0-6.3	~0-4.5	-	< 3	none	-	-	Fewer particles are formed at higher NO_2 conditions.	(Perraud et al., 2012)
	47±3	0-9.6	~0-8.7	294±2	< 1	none	-	-	Particle number concentration and volume were substantially reduced in the presence of NO_2.	(Nøjgaard et al., 2006)
β-pinene	300-1100	~0-6.7	0-4.2	295	23-40	none	-	-	SOA yields are comparable over oxidant conditions studied.	(Draper et al., 2015)
Δ-carene	220-650	~0-3	0-1.9	294-295	27-38	none	-	-	SOA yields are comparable over oxidant conditions studied.	(Draper et al., 2015)
limonene	150-159	0.2-0.4	0.5-75.9	295-297	9.2-9.9	none	30.3-157.3	0.27-0.73	The highest SOA yield occurred when $[O_3]/[NO]$ is around 1.	(Chen et al., 2017)
	300-560	~0-3.3	0-2.2	295	20-31	none	-	-	SOA formation was enhanced at higher NO_2.	(Draper et al., 2015)
	51±3	0-6.9	0-7.1	294±2	< 1	none	-	-	Particle number concentrations were lower at higher NOx conditions.	(Nøjgaard et al., 2006)
γ-terpene	152-154	0-2.9	0-0.7	297-301	24-30	none	-	0.38-0.77	NOx enhance SOA yields and decrease particle number concentrations.	(Xu et al., 2020)

1606 Table 3. Summary of gaseous and particulate species in different regions with anthropogenic-biogenic interactions in China.

Location	Period	T (°C)	RH (%)	SO_2 [a] ($\mu g\ m^{-3}$)	NOx [a] ($\mu g\ m^{-3}$)	NO_3^- [a] ($\mu g\ m^{-3}$)	SO_4^{2-} [a] ($\mu g\ m^{-3}$)	NH_4^+ [a] ($\mu g\ m^{-3}$)	SOA_I Tracers [b]	$\sum SOA_I$ [c] ($ng\ m^{-3}$)	SOA_M Tracers [d]	$\sum SOA_M$ [e] ($ng\ m^{-3}$)	LWC [f] ($\mu g\ m^{-3}$)	pH [g]	References
Guangzhou (urban)	Year 2015	24.0	58	15.1	76.8	3.2	8.4	4.0	2-MT, 2-MG, C5-alkene triols, and 3-MeTHF-3,4-diols	22.6	*cis*-pinonic acid, pinic acid, 3-HGA, HDMGA, MBTCA	50.0	-	-	(Zhang et al., 2019b)
Zhaoqing (urban)	Year 2015	22.7	59	25.5	40.3	4.2	10.0	5.0		49.3		54.3	-	-	
Dongguan (urban)	Year 2015	24.9	61	16.2	49.0	2.9	8.5	3.4		16.0		50.9	-	-	
Nansha (sub-urban)	Year 2015	25.6	67	14.4	38.3	1.8	8.3	3.7		17.0		26.5	-	-	
Zhuhai (sub-urban)	Year 2015	24.2	74	7.3	57.4	1.4	8.5	3.3		10.8		40.3	-	-	
Nanjing (urban)	Summer 2013	32.4	59.7	128 [i]	39.3 [h]	-	17	-	2-MT, 2-MG, and C5-alkene triols	0.3	-	-	70	2.6	(Zhang et al., 2017c)
Beijing (urban)	Summer 2017	16-38	-	-	225 [i]	-	-	-	2-MT, 2-MT OSs, 2-MG, 2-MG OSs, glycolic acid sulfate, hydroxyacetone sulfate, lactic acid sulfate, cyclic, and 9 NOSs	107	-	-	-	-	(Bryant et al., 2020)
Wangqingshan (forest)	Summer 2010	29.6	79.7	29.4	42.4 [h]	2.8	9.1	3.1	2-MT sulfate ester, 2-MG sulfate ester	0.68	*cis*-pinonic acid, pinic acid, 3-HGA, HDMGA, MBTCA, NOSs (three isomers of MW 295)	75.9			(He et al., 2014)
	Fall 2010	21.6	69.1	45.1	37.5	10.4	18.6	8.8		0.66		205.4			

Wangqingshan (forest)	Summer 2008	29.0	66	-	-	5.3	23.0	4.9	3-MeTHF-3,4-diols, 2-MT, C5-alkene triols, 2-MT sulfate ester, 2-MG, 2-MG sulfate ester	130.1	-	-	24.5	0.5	(He et al., 2018)
	Fall 2008	22.6	47	-	-	8.9	15.9	5.3		26.7		-	11.8	2.8	
Mountain Wuyi	Spring 2014	16	78	1.7	4.2 [h]	-	-	-	3-MeTHF-3,4-diols, C5-alkene triols, 2-MT, 2-MG	6.6	*cis*-pinic acid, *cis*-pinonic acid, 3-HGA, MBTCA	26	9.7	0.2	(Ren et al., 2019)
	Summer 2014	23	79	0.9	1.7 [h]	-	-	-		21		36	7.4	0.1	
	Autumn 2014	17	75	3.1	4	-	-	-		16		36	10.8	0.7	
	Winter 2014	6.4	64	6.7	6.2	-	-	-		3		20	7.2	1.6	
Qinghai Lake	Summer 2012	11	59	-	-	0.4	2.2	0.4	3-MeTHF-3,4-diols, C5-alkene triols, 2-MT	3.8	*cis*-pinic acid, *cis*-pinonic acid, 3-HGA, MBTCA	16	-	-	(Ren et al., 2018)
	Winter 2012	-9	26	-	-	0.8	2.2	0.1		0.6		1.3	-	-	
Urumqi (urban)	Summer 2012	26	46	-	-	3.4	6.4	0.4		10		44	-	-	
	Winter 2012	-14	78	-	-	19	65	21		1.9		6.6	-	-	
Xi'an (urban)	Summer 2012	24	78	-	-	8.8	15	4.3		20		58	-	-	
	Winter 2012	1	66	-	-	26	36	13		2.1		22	-	-	
Shanghai (urban)	Summer 2012	28	78	-	-	4.2	7.2	1.3		5.1		20	-	-	
	Winter 2012	6	70	-	-	16	16	6.1		2.5		16	-	-	
Chengdu (urban)	Summer 2012	25	81	-	-	6.5	14	3.4		23		88	-	-	
	Winter 2012	10	74	-	-	26	32	12		5.9		17	-	-	
Guangzhou (urban)	Summer 2012	29	79	-	-	3.3	6.2	0.8		10		43	-	-	
	Winter 2012	17	73	-	-	12	15	5.1		6		46	-	-	
Tibetan Plateau (Qinghai	Summer 2010	14.4	64.4	-	-	0.8	3.9	0.6	C5-alkene triols, 2-MG, 2-MT	2.5	norpinic acid, pinonic acid, pinic acid, 3-HGA, MBTCA	3.0	5.8	-1.2	(Li et al., 2013)

Lake)															
Changbai Mountain	Summer, 2007	25	59	5.35	1.3	-	-	-	2-MT, 2-MG, C5-alkene triols	53	pinic acid, norpinic acid, 3-HGA, MBTCA	31	-	-	(Wang et al., 2008)
Chongming Island	Summer 2006	29	68	25.9	40.9 [j]	-	-	-		4.8		1.8	-	-	

[a] The mean concentration of tracers; [b] Isoprene-derived SOA (SOA_I) tracers: 2-MG (2-methylglyceric acid), 2-MT (2-methyltetrols that represent the sum of 2-methylthreitol and 2-methylerythritol), 3-MeTHF-3,4-diols (the sum of *trans*-3-methyltetrahydrofuran-3,4-diol and *cis*-3-methyltetrahydrofuran-3,4-diol), C5-alkene triols (the sum of *cis*-2-methyl-1,3,4-trihydoxy-1-butane, *trans*-2-methyl-1,3,4-trihydoxy-1-butane, and 3-methyl-2,3,4-trihydoxy-1-butane), OSs (organosulfates), NOSs (nitrooxy organosulfates); [c] The sum of SOA_I tracers; [d] Monoterpene-derived SOA (SOA_M) tracers: 3-HGA (3-hydroxyglutaric acid), HDMGA (3-Hydroxy-4,4-dimethylglutaric acid), MBTCA (3-methyl-1,2,3-butanetricarboxylic acid); [e] The sum of SOA_M tracers; [f] Aerosol liquid water content; [g] AIM-derived in situ pH of the aqueous phase on aerosols; [h] The concentration of NO_2; [i] The max concentration.

1612 **Figures**

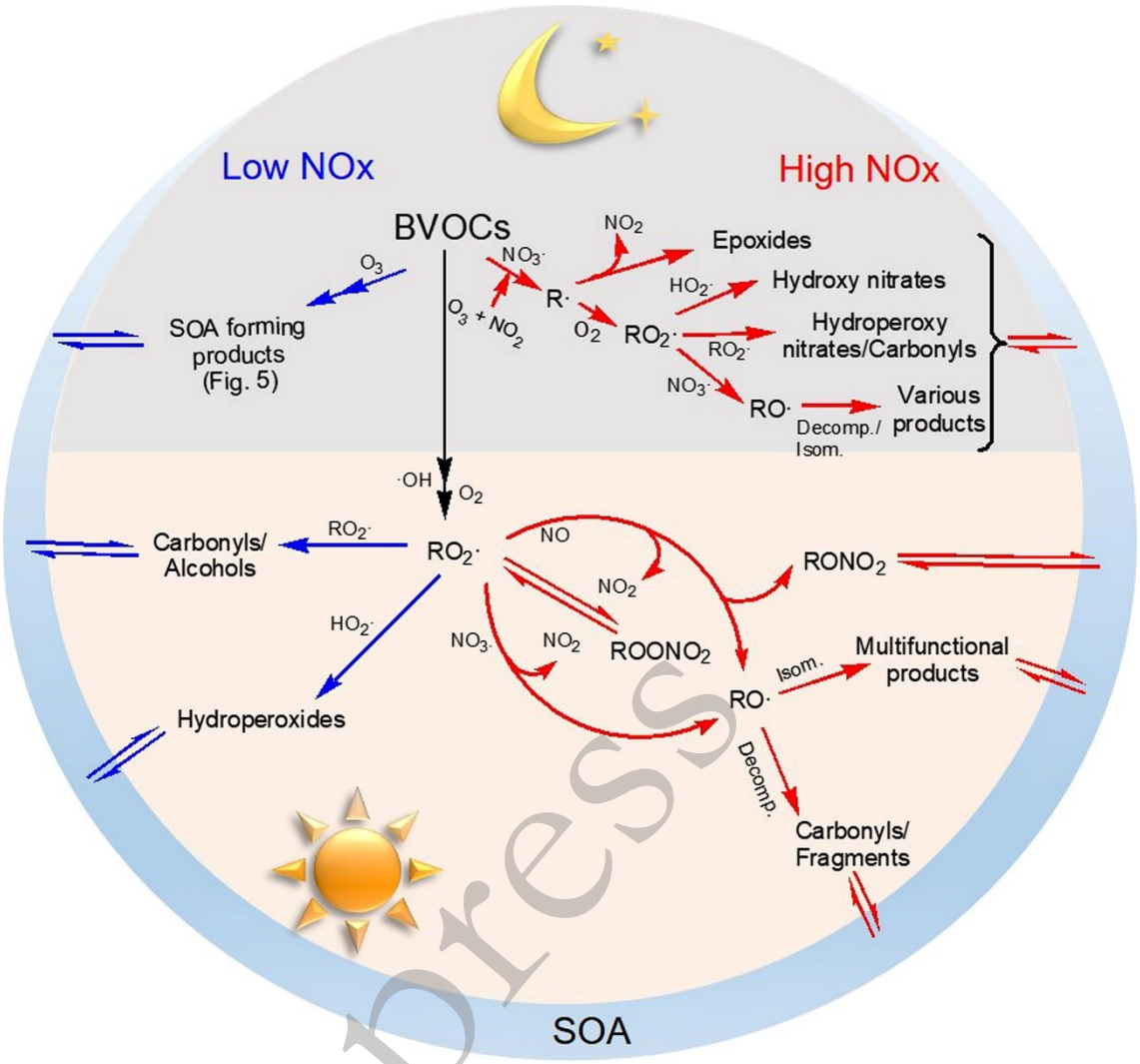

1613
1614
1615 **Fig. 1.** General schematic picture of NOx effects on BVOCs oxidation during daytime
1616 and nighttime. 'Decom.' and 'Isom.' represents decomposition and isomerization
1617 reactions, respectively.

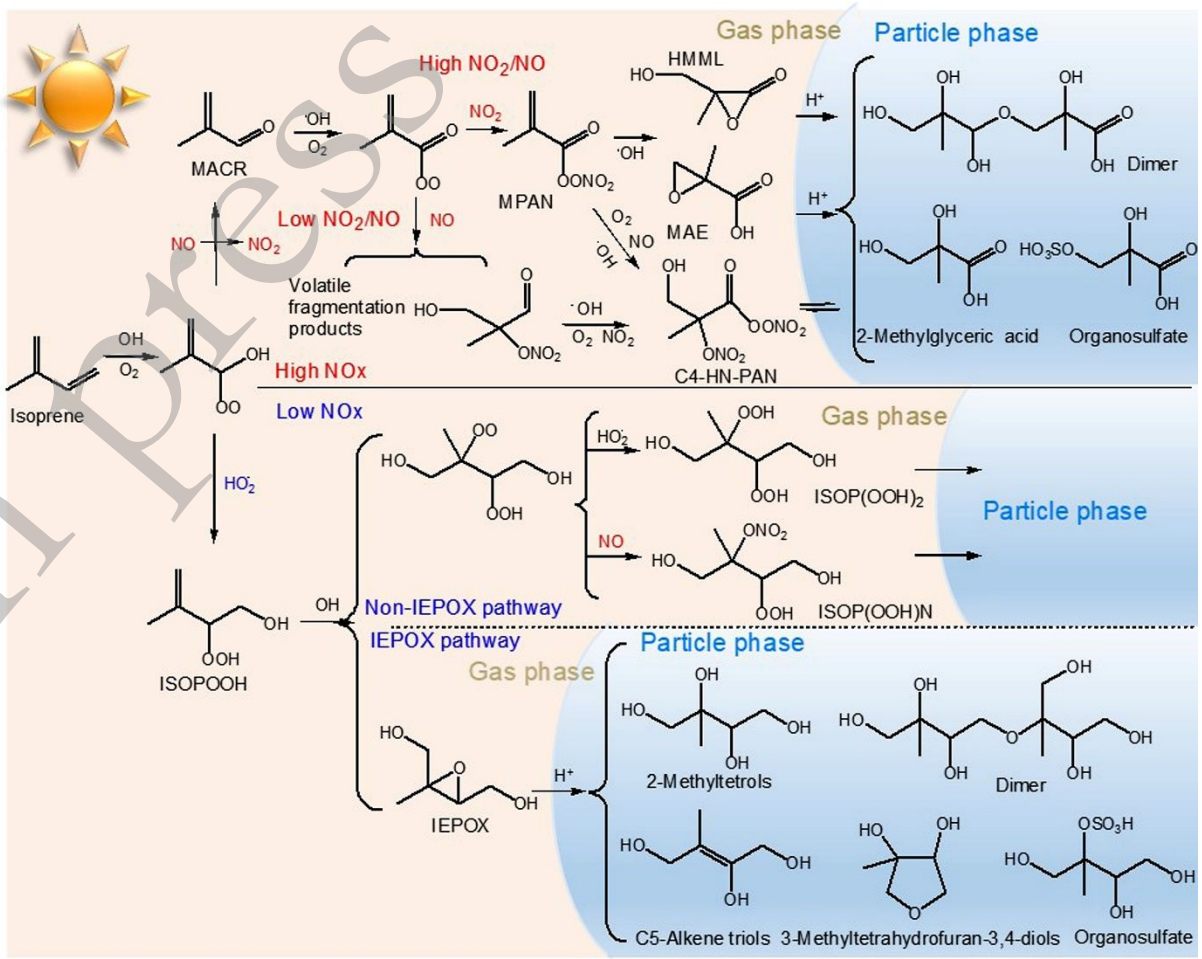

Fig. 2. Effects of NOx on isoprene SOA formation during daytime. Under high NOx conditions, isoprene $RO_2\cdot$ primarily reacts with NO, forming methacrolein (MACR). The oxidation of MACR under high NO_2/NO ratios forms methacryloylperoxynitrate (MPAN) while C4-hydroxynitrate

peroxyacyl nitrate (C4-HN-PAN) is the main intermediate leading to SOA under high NOx condition with low NO_2/NO ratios. MPAN further reacts with ·OH to form methacrylic epoxide (MAE) and hydroxymethylmethyl-α-lactone (HMML). Acid-catalyzed reactions of MAE in the particle-phase produce 2-methylglyceric acid, an organosulfate, and an oligomer. Under low NOx conditions, isoprene RO_2· reacts predominantly with HO_2·, leading to hydroxy hydroperoxide (ISOPOOH). ISOPOOH-derived epoxydiols (IEPOX) undergo multiphase acid-catalyzed chemistry to give various products in the particle-phase. The none-IEPOX pathway that gives dihydroxy dihydroperoxides ($ISOP(OOH)_2$) and organic nitrates (ISOP(OOH)N) is proposed to contribute to SOA formation without reactive aqueous seed particles. References for the none-IEPOX pathways are Liu et al. (2016) and Riva et al. (2016c) while for other pathways are Lin et al. (2013b), Surratt et al. (2010); Lin et al. (2012); Lin et al. (2013a).

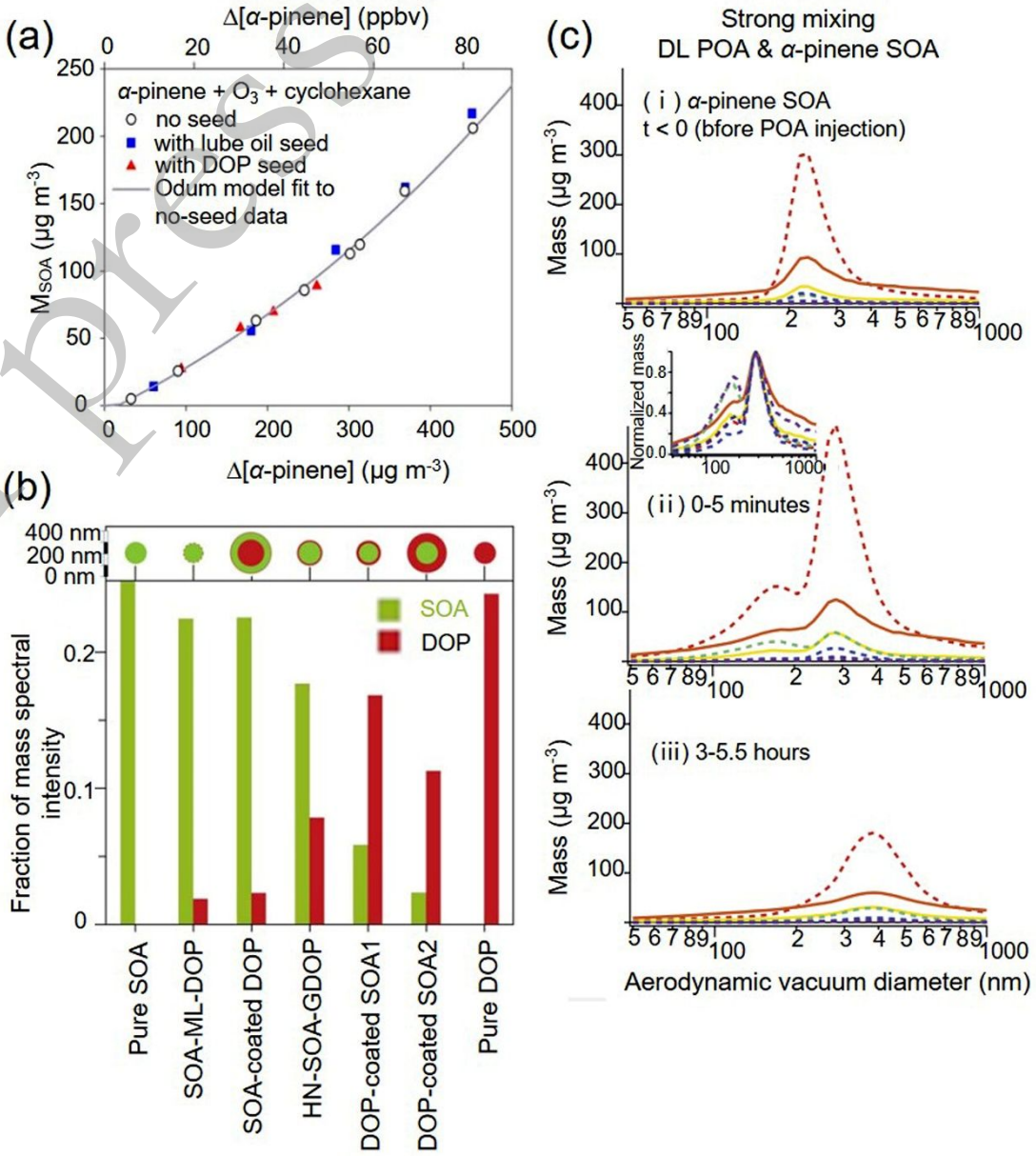
(a)
Δ[α-pinene] (ppbv)
α-pinene + O3 + cyclohexane
no seed
with lube oil seed
with DOP seed
Odum model fit to no-seed data
MSOA (μg m-3)
Δ[α-pinene] (μg m-3)
(b)
400 nm
200 nm
0 nm
SOA
DOP
Fraction of mass spectral intensity
Pure SOA
SOA-ML-DOP
SOA-coated DOP
HN-SOA-GDOP
DOP-coated SOA1
DOP-coated SOA2
Pure DOP
(c)
Strong mixing
DL POA & α-pinene SOA
(i) α-pinene SOA
t < 0 (bfore POA injection)
Normalized mass
(ii) 0-5 minutes
(iii) 3-5.5 hours
Mass (μg m-3)
Aerodynamic vacuum diameter (nm)

Fig. 3. The mixing behavior of α-pinene SOA with anthropogenic POA. (a) Dioctyl phthalate (DOP) and lubricating oil seeds exhibited no influence on SOA mass formation from α-pinene ozonolysis (Adapted from Song et al. (2007)). (b) Relative MS intensity of DOP and SOA for different types of particles under the same laser power. High MS intensity of surface material was observed, indicating the phase-separation between α-pinene and DOP (Adapted from Vaden et al. (2010). (c) A single-phase mixture formed between DOP seed and α-pinene SOA (Adapted from Asa-Awuku et al. (2009)).

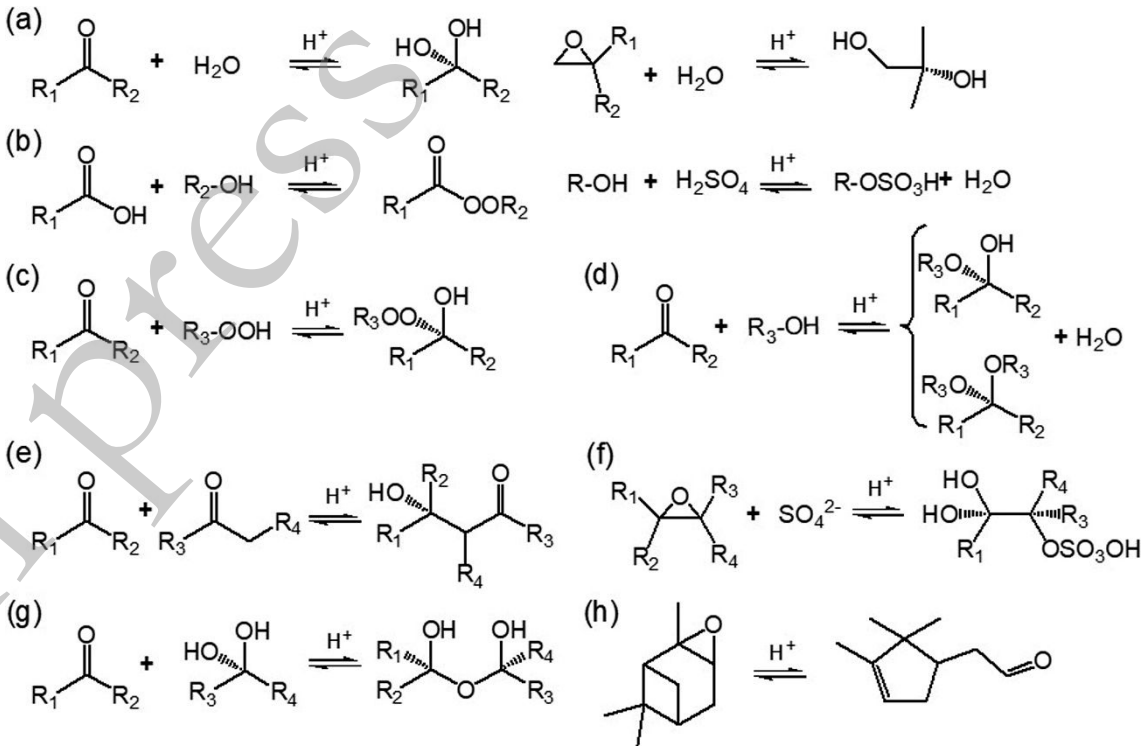

Fig. 4. Acid-catalyzed particle-phase reactions that might affect the volatility of organics from BVOCs oxidation. (a) Hydration reactions of carbonyl and epoxide. (b) Esterification between alcohol and carboxylic acid and/or sulfuric acid. (c) Peroxyhemiacetal formation via the reaction between hydroperoxide and aldehyde. (d) Hemiacetal or acetal formation via the reaction between aldehyde and alcohol. (e) Aldol condensation reaction between two carbonyls. (f) Organosulfates formation via nucleophilic addition reaction. (g) Polymerization. (h) Isomerization. References of these reactions include (Kroll and Seinfeld, 2008; Hallquist et al., 2009; Darer et al., 2011; Ziemann and Atkinson, 2012; Iinuma et al., 2013).

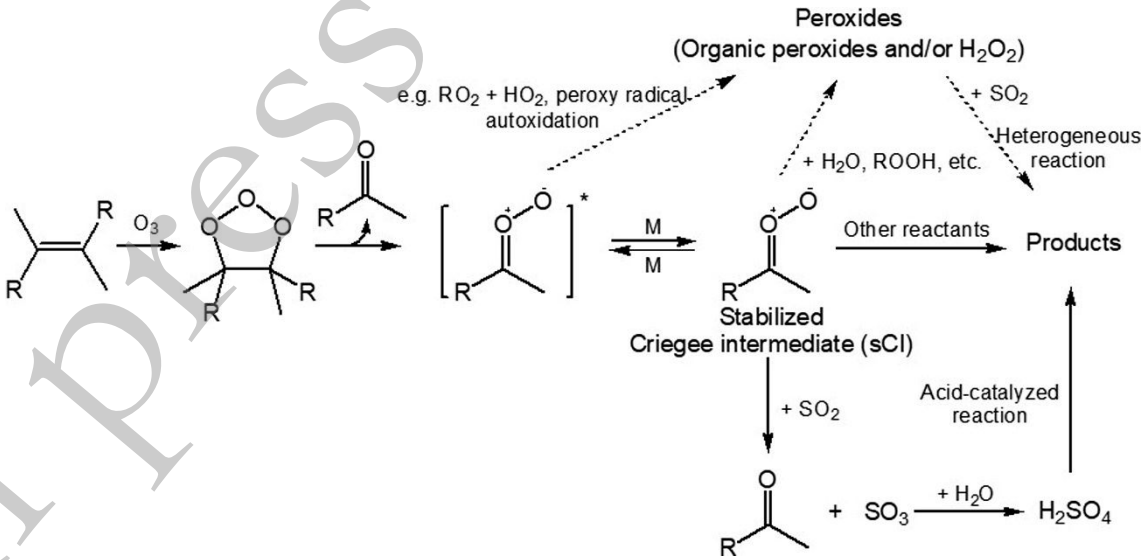

Fig. 5. SO_2 effects on the formation of SOA from monoterpene ozonolysis: sCIs + SO_2, sCIs + H_2O, and SO_2 + peroxides reactions (Adapted from Ye et al. (2018)].

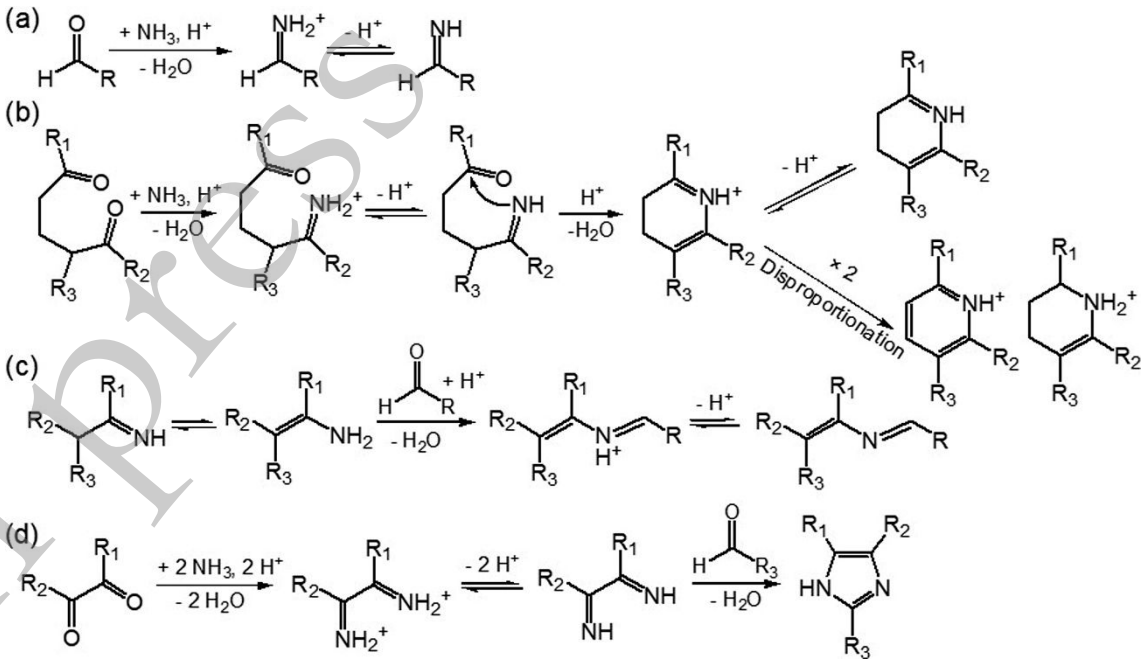

Fig. 6. Aging pathways of biogenic SOA by ammonia. (a) Acid-catalyzed reaction of carbonyls with ammonia that results in the formation of primary imines (Moise et al. (2015) and reference therein). (b) The reaction between ammonia and 1,5-dicarbonyl compounds: the primary imine can further react with the second carbonyl group present in the same molecule through nucleophilic addition, resulting in nitrogen-containing heterocyclic compounds (Moise et al. (2015) and reference therein). (c) Reactions between the primary imine with another carbonyl group, leading to a more stable secondary imine (Schiff base) (Moise et al. (2015) and reference therein). (d) The reaction between ammonia and 1,2-dicarbonyls through a Debus reaction, yielding substituted imidazoles (Updyke et al., 2012).

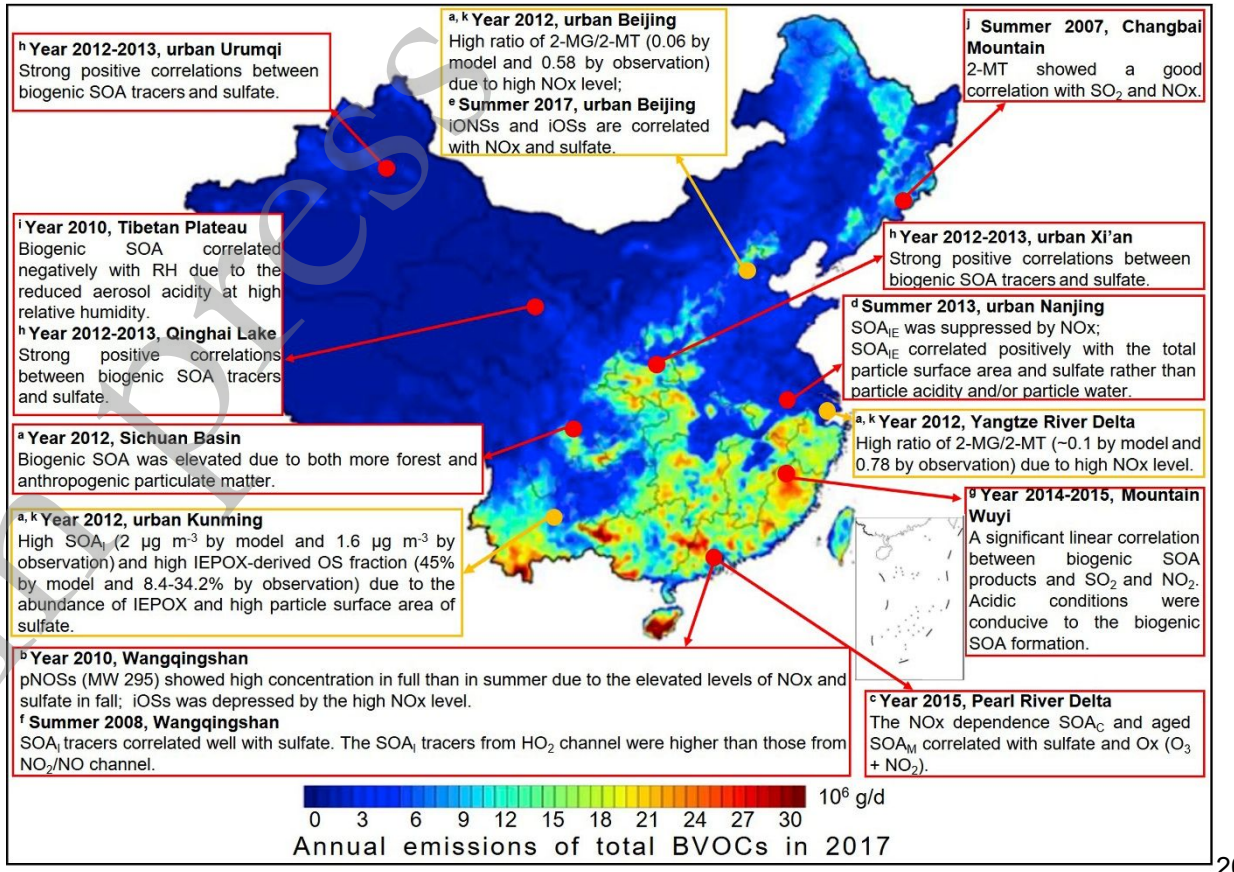

Fig. 7. Anthropogenic-biogenic interactions in China. The color mapped annual emissions of total BVOCs in China, 2017, is adapted from Wu et al. (2020). The observed correlations between anthropogenic pollutants and biogenic SOA are shown in red boxes and the modelled results are shown in yellow boxes. The pONSs, iONSs, iOSs, SOA_I, SOA_{IE}, SOA_M, and SOA_C refer to pinene-derived nitrooxyorganosulfates, isoprene-

derived nitrooxyorganosulfates, isoprene-derived organosulfates, isoprene-derived SOA, IEPOX-derived SOA, monoterpene-derived SOA and *β*-caryophyllene-derived SOA respectively; 2-MG and 2-MT are 2-methylglyceric acid and 2-methyltetrols derived from isoprene oxidation under high- and low-NOx conditions, respectively. [a] The modelled anthropogenic-biogenic interactions are taken from Qin et al. (2018). [b-j] The field observed anthropogenic-biogenic interactions are taken from He et al. (2014), Zhang et al. (2019), Zhang et al. (2017), Bryant et al. (2019), He et al. (2018), Ren et al. (2019), Ren et al. (2018), Li et al. (2013), Wang et al. (2008), respectively.